To involvement the conformation of the adenine nucleotide translocase in opening the Tl+-induced permeability transition pore in Ca2+-loaded rat liver mitochondria

Korotkov, Sergey M.

2016-04

Korotkov , S M , Konovalova , S A , Brailovskaya , I V & Saris , N-E L 2016 , ' To involvement the conformation of the adenine nucleotide translocase in opening the Tl+-induced permeability transition pore in Ca2+-loaded rat liver mitochondria ' , Toxicology in Vitro , vol. 32 , pp. 320-332 . https://doi.org/10.1016/j.tiv.2016.01.015

http://hdl.handle.net/10138/233305
https://doi.org/10.1016/j.tiv.2016.01.015

publishedVersion

Toxicology in Vitro 32 (2016) 320–332

Contents lists available at ScienceDirect

Toxicology in Vitro

journal homepage: www.elsevier.com/locate/toxinvit

To involvement the conformation of the adenine nucleotide translocase in opening the Tl^+-induced permeability transition pore in Ca^{2+}-loaded rat liver mitochondria

Sergey M. Korotkov [a,*], Svetlana A. Konovalova [a], Irina V. Brailovskaya [a], Nils-Erik L. Saris [b]

[a] Sechenov Institute of Evolutionary Physiology and Biochemistry, the Russian Academy of Sciences, Thorez pr. 44, 194223 St. Petersburg, Russian Federation
[b] Department of Food and Environmental Sciences, University of Helsinki, P.O. Box 56, Viikki Biocenter 1, FI-00014 Helsinki, Finland

ARTICLE INFO

Article history:
Received 14 June 2015
Received in revised form 5 January 2016
Accepted 29 January 2016
Available online 4 February 2016

Keywords:
Tl^+
Ca^{2+}
Mitochondrial permeability transition
Adenine nucleotide translocase conformation
Mitochondrial swelling
Rat liver mitochondria

ABSTRACT

The conformation of adenine nucleotide translocase (ANT) has a profound impact in opening the mitochondrial permeability transition pore (MPTP) in the inner membrane. Fixing the ANT in 'c' conformation by phenylarsine oxide (PAO), *tert*-butylhydroperoxide (tBHP), and carboxyatractyloside as well as the interaction of 4,4′-diisothiocyanostilbene-2,2′-disulfonate (DIDS) with mitochondrial thiols markedly attenuated the ability of ADP to inhibit the MPTP opening. We earlier found (Korotkov and Saris, 2011) that calcium load of rat liver mitochondria in medium containing $TlNO_3$ and KNO_3 stimulated the Tl^+-induced MPTP opening in the inner mitochondrial membrane. The MPTP opening as well as followed increase in swelling, a drop in membrane potential ($\Delta\Psi_{mito}$), and a decrease in state 3, state 4, and 2,4-dinitrophenol-uncoupled respiration were visibly enhanced in the presence of PAO, tBHP, DIDS, and carboxyatractyloside. However, these effects were markedly inhibited by ADP and membrane-penetrant hydrophobic thiol reagent, N-ethylmaleimide (NEM) which fix the ANT in 'm' conformation. Cyclosporine A additionally potentiated these effects of ADP and NEM. Our data suggest that conformational changes of the ANT may be directly involved in the opening of the Tl^+-induced MPTP in the inner membrane of Ca^{2+}-loaded rat liver mitochondria. Using the Tl^+-induced MPTP model is discussed in terms finding new transition pore inhibitors and inducers among different chemical and natural compounds.

1. Introduction

It is known that the opening of the MPTP occurs in response to Ca^{2+} overload, especially when accompanied by oxidative stress, raised inorganic phosphate concentration and adenine nucleotide depletion in the mitochondrial matrix (Halestrap, 2010). It has recently been suggested that the PiC and the CyP-D are the main structural parts of the MPTP, whereas the ANT interacting closely with the first two could be attributed to the regulatory component of the pore (Baines, 2009; Halestrap, 2010; Elrod and Molkentin, 2013; Gutiérrez-Aguilar and Baines, 2015). Presently, appearance of the large multiprotein complex, MPTP in the IMM is inferred by a new model which suggests that CypD is bonded to the PiC and the ANT, and also interacts with the lateral stalk or *c*-subunit of ATP-synthase to regulate CsA-dependent pore opening in Ca^{2+}-loaded mitochondria (Giorgio et al., 2009; Bernardi, 2013; Bonora et al., 2013; Chinopoulos and Szabadkai, 2013; Elrod and Molkentin, 2013; Giorgio et al., 2013; Gutiérrez-Aguilar and Baines, 2015; Bonora et al., 2015). The MPTP is regulated by adenine nucleotides, $\Delta\Psi_{mito}$, and the ANT ligands (ADP, CATR, and BKA) (Halestrap and Brenner, 2003; Halestrap, 2010). Involvement of the ANT in pore formation is suggested by the stimulation of MPTP opening by stress inductors (tBHP and diamide), thiol cross-linker PAO, and CATR which stabilize the ANT in 'c' conformation, increasing Cyp-D binding and reducing ADP binding with specific sites of the translocase (Petronilli et al., 1994; Castilho et al., 1996; McStay et al., 2002; Halestrap and Brenner, 2003; Halestrap, 2010). Experiments with mersalyl and bifunctional reagent DIDS revealed that conformational changes are involved in altering the reactivity of the ANT thiol groups (Bernardes et al., 1994; Lapidus and Sokolove, 1994; Bernardes et al., 1997; Kowaltowski et al., 1997). ADP, NEM, EMA and thiol-specific dimaleimides fix the ANT in 'm' conformation, and as a result, decreased affinity of the calcium binding site to Ca^{2+} and the MPTP inhibition,

Abbreviations: MPTP, mitochondrial permeability transition pore; PiC, mitochondrial phosphate carrier; CyP-D, cyclophilin D; ANT, adenine nucleotide translocase; IMM, inner mitochondrial membrane; CsA, cyclosporine A; $\Delta\Psi_{mito}$, mitochondrial membrane potential; CATR, carboxyatractyloside; BKA, bongkrekic acid; tBHP, tert-butylhydroperoxide; PAO, phenylarsine oxide; DIDS, 4,4′-Diisothiocyanostilbene-2,2′-disulfonate; NEM, N-ethylmaleimide; EMA, eosin-5-maleimide; CaRLM, Ca^{2+}-loaded rat liver mitochondria; DNP, 2,4-dinitrophenol; EGTA, ethylene glycol-bis(β-aminoethyl ether) N,N,N′,N′-tetraacetic acid; RCR_{ADP}, respiratory control ratio; RCR_{DNP}, DNP-dependent respiratory control ratio; RLM, rat liver mitochondria; ROS, reactive oxygen species; MSL, mersalyl; DTT, dithiothreitol; FCCP, carbonyl cyanide 4-(trifluoromethoxy)phenylhydrazone; PSSG, glutathionylated proteins.

* Corresponding author at: Sechenov Institute of Evolutionary Physiology and Biochemistry, the Russian Academy of Sciences, Thorez pr. 44, 194223 St. Petersburg, Russian Federation.
E-mail address: korotkov@SK1645.spb.edu (S.M. Korotkov).

http://dx.doi.org/10.1016/j.tiv.2016.01.015
0887-2333/

followed by mitochondrial swelling and $\Delta\Psi_{mito}$ disruption had place in experiments with tBHP, diamide, arsenite, or menadione (Majima et al., 1993; Petronilli et al., 1994; Kowaltowski et al., 1997; Hashimoto et al., 1999; McStay et al., 2002; Halestrap and Brenner, 2003; Nantes et al., 2011).

Experiments in which swelling of RLM occurred in nitrate media showed that the IMM has a low permeability to K^+ but a higher permeability to Tl^+ (Brierley et al., 1970; Saris et al., 1981; Korotkov et al., 2008). The opening of the Tl^+-induced MPTP in IMM of CaRLM was observed in medium containing 25–75 mM $TlNO_3$, KNO_3, and 25–100 μM Ca^{2+} (Korotkov and Saris, 2011). This opening was accompanied by increased mitochondrial swelling and $\Delta\Psi_{mito}$ dissipation, as well as a decrease in state 4, state 3 and DNP-uncoupled respiration of the mitochondria (Korotkov and Saris, 2011). These effects were markedly decreased by the MPTP inhibitors (ADP and CsA). On the other hand, cytotoxic effects of Tl^+ in experiments with isolated rat hepatocytes (Pourahmad et al., 2010) were considerably reduced by the MPTP inhibitors (CsA and carnitine). We recently demonstrated that Tl^+ interacted only weakly with the IMM thiol groups, but formed complexes with soluble matrix proteins of RLM in medium containing $TlNO_3$ and KNO_3 (Korotkov et al., 2014a). The swelling of non-energized RLM in the medium was decreased by ADP in experiments with Y^{3+} and La^{3+} (Korotkov et al., 2014b) or Tl^+ alone (Korotkov and Saris, 2011) which points to the possible participation of the ANT in regulating the inner membrane ion permeability to Tl^+ ions. At the same time, we are still uncertain about the involvement of conformational changes of the ANT at opening of the Tl^+-induced MPTP. Our aim was therefore to study the influence of reagents (PAO, DIDS, tBHP, and CATR), fixing the ANT 'c' conformation, on the ability of ADP, BKA and NEM, fixing the ANT 'm' conformation, to inhibit the Tl^+-induced MPTP opening in the inner membrane of CaRLM. We investigated influence of these reagents on swelling, basal, state 4, state 3 and DNP-uncoupled respiration, and $\Delta\Psi_{mito}$ dissipation of CaRLM, injected into medium containing $TlNO_3$, KNO_3, succinate, and rotenone.

2. Materials and methods

2.1. Animals

The research was used male Wistar rats (250–300 g) which were kept at 20–23 °C under 12-h light/dark cycle with free access to water ad libitum and the standard rat diet. All treatment procedures of animals were carried out according to the Animal Welfare act and the Institute Guide for Care and Use of Laboratory Animals.

2.2. Isolation of mitochondria

Rat liver mitochondria were isolated according to the standard procedure (Korotkov et al., 2015a). To get pellet containing mitochondria, rat liver was homogenized in a buffer containing 250 mM sucrose, 3 mM Tris–HCl (pH 7.3), and 0.5 mM EGTA and successively centrifuged at 800 ×*g* and 10,000 ×*g*. Next the pellet was rinsed twice by resuspension–centrifugation in a buffer containing 250 mM sucrose and 3 mM Tris–HCl (pH 7.3) and finally suspended in 1 ml of the latter buffer. The protein content in mitochondrial preparations was assayed by Bradford's method and it was within 50–60 mg/ml.

2.3. Swelling of mitochondria

The early mention about the use of millimolar Tl^+ concentrations was made by Melnick et al. (1976) and Saris et al. (1981) which applied swelling and polarographic techniques in experiments with isolated mitochondria. The applicability of such experimental model in toxicological studies in vitro was earlier discussed by us in more detail (Korotkov et al., 2007; Korotkov et al., 2015b). Mitochondrial swelling was measured as a decline in A_{540} at 20 °C using a SF-46 spectrophotometer (LOMO, St. Petersburg, Russia). Mitochondria (1.5 mg protein/ml) were injected into a 1-cm cuvette with 1.5 ml of 400 mOsm medium containing 200 mM KNO_3 (Fig. 1A and C) or 75 mM $TlNO_3$ and 125 mM KNO_3 (Figs. 1B and D, 2–4) as well as 5 mM succinate, 5 mM Tris-NO_3 (pH 7.3), 2 μM rotenone, and 1 μg/ml of oligomycin. The

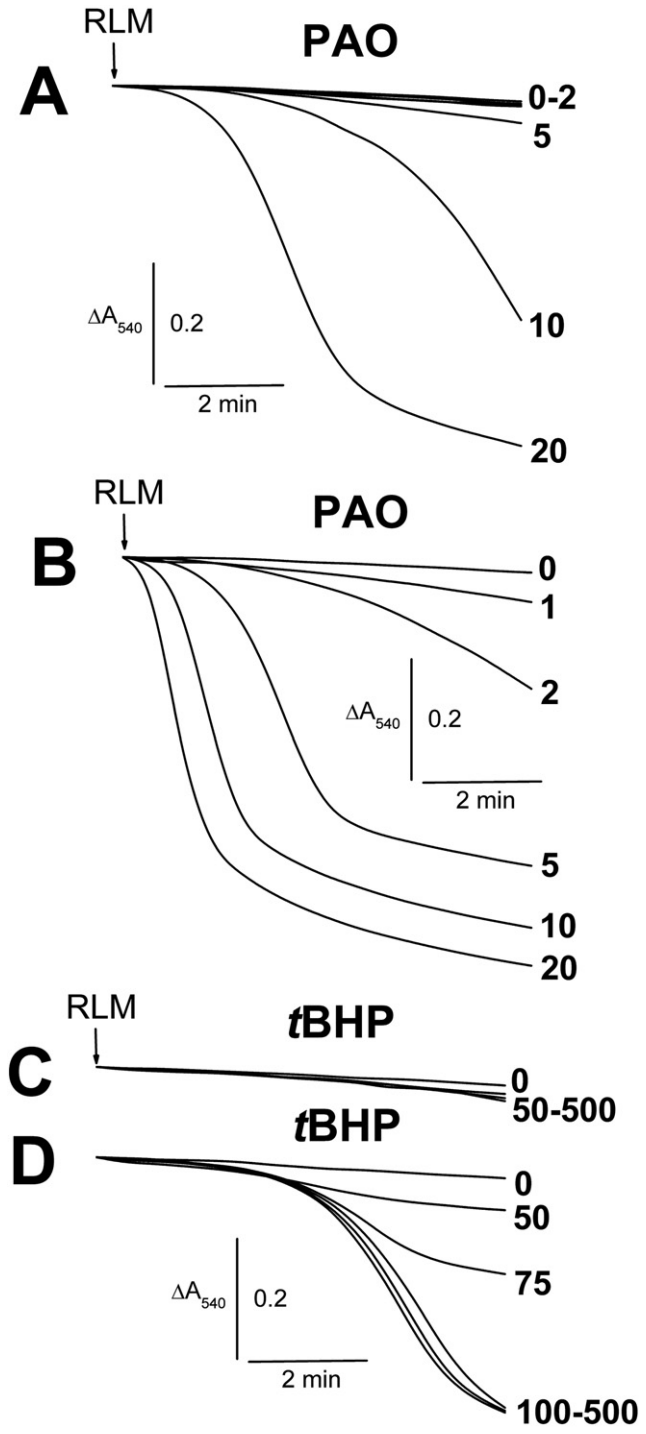

Fig. 1. The influence of PAO and tBHP on swelling of succinate-energized rat liver mitochondria in the nitrate medium. Mitochondria (1.5 mg of protein per ml) were added to the medium containing 200 mM KNO_3 (panels A and C) or 75 mM $TlNO_3$ and 125 mM KNO_3 (panels B and D) as well as 5 mM Tris-succinate, 5 mM Tris-NO_3 (pH 7.3), 2 μM rotenone, and 1 μg/ml of oligomycin. Numbers on the right of the traces show additions (μM), injected before mitochondria, of PAO (panels A and B) and tBHP (panels C and D) in the medium. Addition of mitochondria (RLM) is shown by arrows. The apparent absorbance change (Figs. 1–4) was within 4% ($p < 0.01$). Representative traces from one of three independent experiments are presented. More detailed statistics for the swelling experiments (Figs. 1–4) see Korotkov (2016).

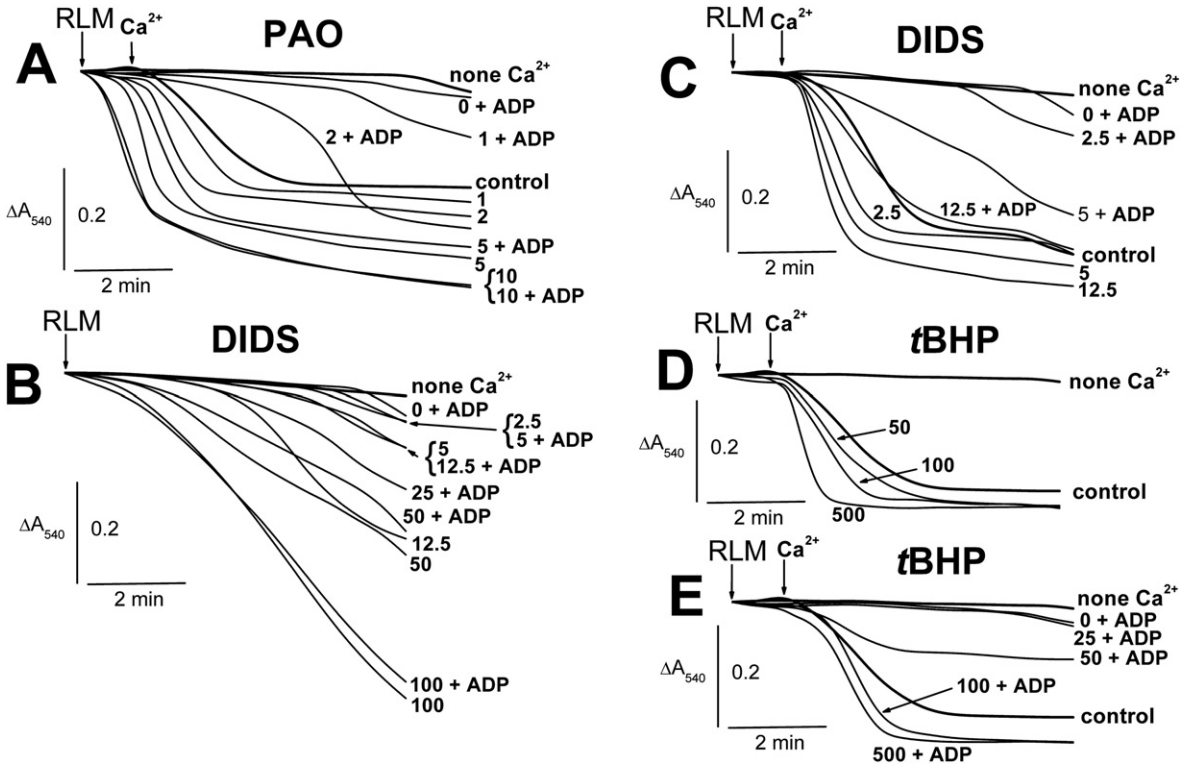

Fig. 2. Effects of PAO, DIDS, tBHP, and Ca^{2+} on Tl^{+}-induced swelling of succinate-energized rat liver mitochondria in the presence of ADP. Mitochondria (1.5 mg/ml of protein) were added to medium containing 75 mM $TlNO_3$, 125 mM KNO_3, 5 mM Tris-succinate, 5 mM Tris-NO_3 (pH 7.3), 2 μM rotenone, and 1 μg/ml of oligomycin. The control trace (in bold) shows swelling of mitochondria after injection of 100 μM Ca^{2+} alone (Figs. 2–4). Additions before mitochondria are indicated to right of traces: free of additions (none Ca^{2+}, in bold) and 500 μM ADP (ADP). Numbers on the right of the traces show additions (μM), administrated before mitochondria, of PAO (panel A), DIDS (panels B and C), and tBHP (panels D and E) in the medium. Additions of mitochondria (RLM) and 100 μM Ca^{2+} (Ca^{2+}) are shown by arrows. Typical traces from one of three independent different mitochondrial preparations are presented.

following chemicals were added into the medium before or after mitochondria (see Figs. 1–4 legends more detail): Ca^{2+}, PAO, tBHP, NEM, DIDS, ADP, CsA, BKA, and CATR. The swelling, oxygen consumption rates, and $\Delta\Psi_{mito}$ were studied in 400 mOsm media in order to verify the comparability and consistency between data in different experiments.

2.4. Oxygen consumption assay

Respiration (oxygen consumption rate) was evaluated polarographically using Expert-001 analyzer (Econix-Expert Ltd., Moscow, Russia) in a 1.3-ml closed thermostatic chamber with magnetic stirring at 26 °C. Mitochondria (1.5 mg protein/ml) were injected to 400 mOsm medium containing 25 mM $TlNO_3$, 100 mM sucrose, 3 mM $Mg(NO_3)_2$, and 3 mM Tris-P_i (Fig. 5) or 75 mM $TlNO_3$ and 1 μg/ml of oligomycin (Fig. 6) as well as 125 mM KNO_3, 5 mM Tris-NO_3 (pH 7.3), 5 mM succinate, and 2 μM rotenone. The following reagents were added in the medium before or after mitochondria: Ca^{2+}, PAO, tBHP, NEM, DIDS, ADP, and CsA (see Figs. 5–6 legends). ADP at 130 μM and DNP at 30 μM were correspondingly administrated into the medium after 2 min recording of state 4 (Fig. 5) or basal state (Figs. 5–6) to induce state 3 and DNP-uncoupled respiration. The respiratory control ratio (RCR_{ADP}) was calculated as a ratio of state 3 to state 4 (Fig. 5 and see Table 5 in Korotkov (2016)). The RCR_{DNP} was accordingly quantified as a ratio of DNP-uncoupled respiration to state 4 (Fig. 5) or a basal state respiration (Fig. 6 and see Table 6 in Korotkov (2016)).

2.5. Mitochondrial membrane potential

The $\Delta\Psi_{mito}$ induced in succinate-energized on the IMM of RLM (Fig. 7) was evaluated according to Waldmeier et al. (2002) by the intensity of safranin fluorescence (arbitrary units) in the mitochondrial suspension with magnetic stirring at 20 °C using a Shimadzu RF-1501 spectrofluorimeter (Shimadzu, Japan) at 485/590 nm wavelength (excitation/emission). Mitochondria (0.5 mg protein/ml) were placed into a quartz cuvette of four clear walls with 3 ml of a medium containing 20 mM $TlNO_3$, 125 mM KNO_3, 110 mM sucrose, 5 mM Tris-NO_3 (pH 7.3), 1 mM Tris-P_i, 3 μM safranin, 2 μM rotenone, and 1 μg/ml of oligomycin. In addition, the next chemicals were added in the medium before mitochondria: PAO, tBHP, DIDS, ADP, and CsA (where indicated). Succinate, Ca^{2+}, and DNP were administrated into the medium after mitochondria (see Fig. 7 legend). Temperature conditions used in the research (Figs. 1–7) were standard for experiments with isolated mitochondria in vitro.

2.6. Statistics

The statistical differences in results and corresponding *p*-values were evaluated using two population *t*-test (Microcal Origin, Version 6.0, Microcal Software). These differences are presented as percent of the average ($p < 0.05$) from one of three independent experiments (Figs. 1–7). More detailed statistical analysis, see in Korotkov (2016).

2.7. Chemicals

$CaCl_2$, $Mg(NO_3)_2$, H_3PO_4, KNO_3, $TlNO_3$, and DNP were of analytical grade from Nevareactiv (St. Petersburg, Russia). Rotenone, oligomycin, PAO, tBHP, NEM, tris-OH, EGTA, ADP, CsA, BKA, CATR, and succinate were from Sigma (St. Louis, MO, USA). DIDS was purchased from Santa Cruz Biotechnology (USA). Sucrose as 1 M solution was refined from cation traces on a column filled with a KU-2-8 resin from Azot (Kemerovo, Russia).

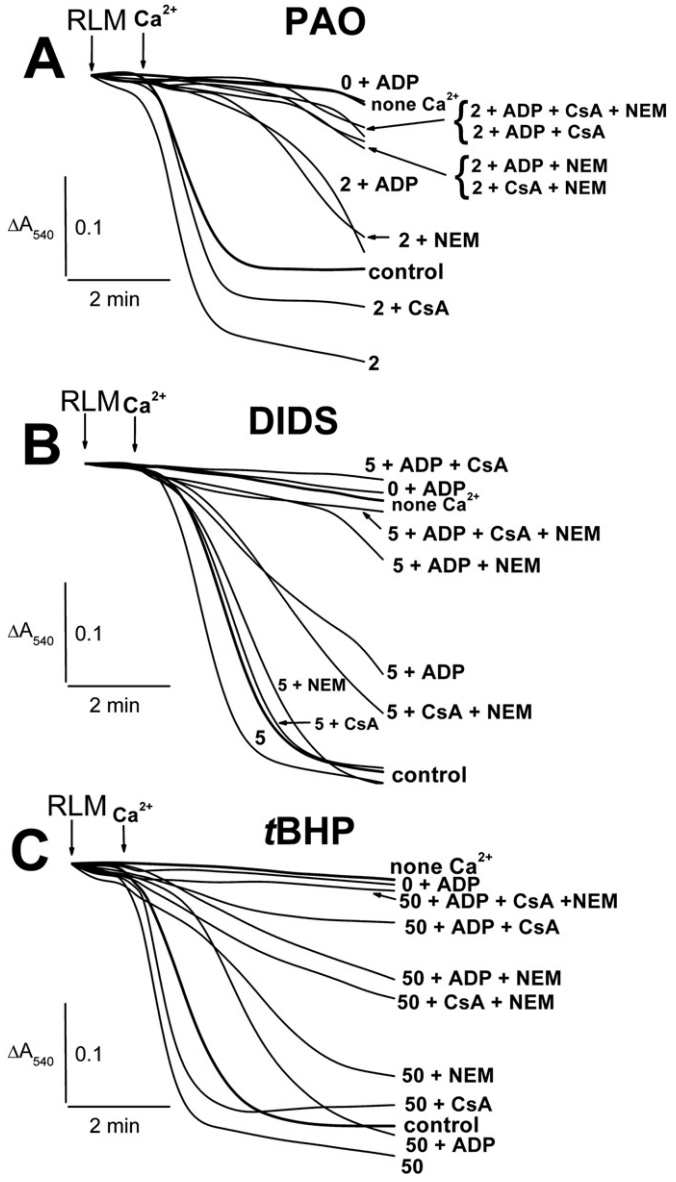

Fig. 3. Effects of PAO, DIDS, tBHP, and Ca^{2+} on Tl^{+}-induced swelling of succinate-energized rat liver mitochondria in the presence of ADP, CsA, NEM, and Mg^{2+}. Mitochondria (1.5 mg/ml of protein) were added to medium like one of Fig. 2. Additions before mitochondria are indicated to right of traces: free of additions (none Ca^{2+}, in bold), 500 μM ADP (ADP), 1 μM CsA (CsA), and 50 μM NEM (NEM). Numbers on the right of the traces show additions (μM), added before mitochondria, of PAO (panel A), DIDS (panel B), and tBHP (panel C) in the medium. Additions of mitochondria (RLM) and 100 μM Ca^{2+} (Ca^{2+}) are shown by arrows. Typical traces from one of three different mitochondrial preparations are presented.

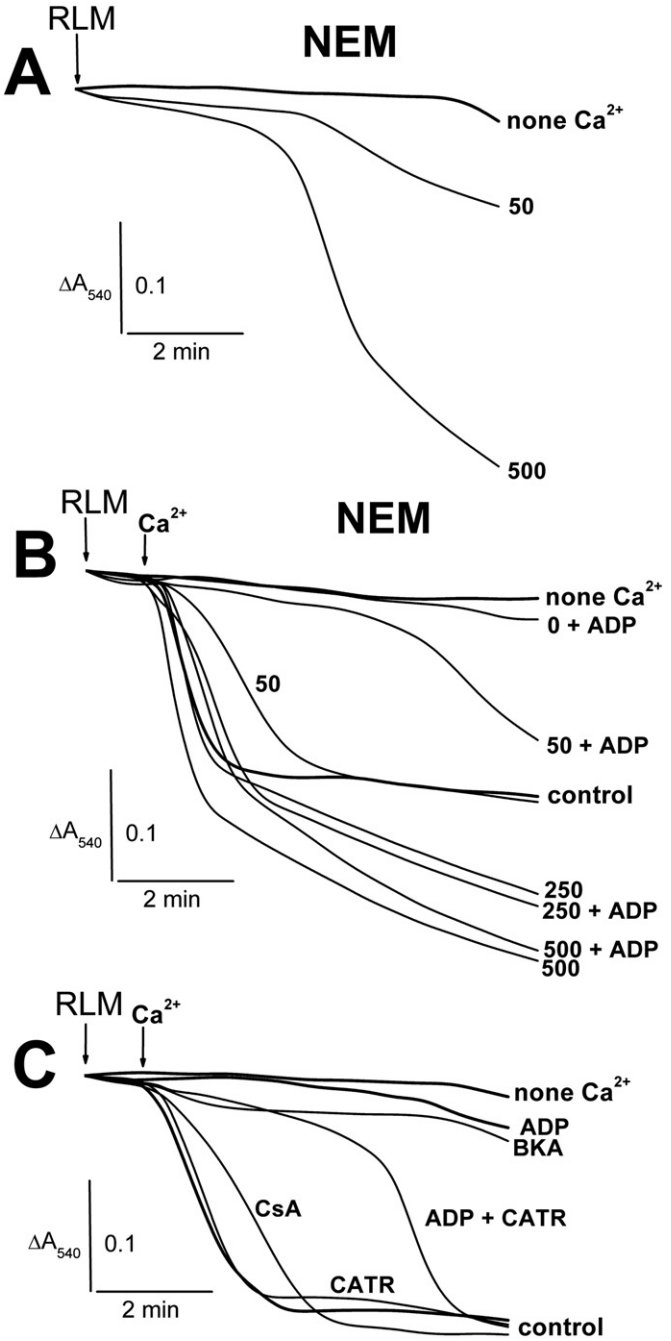

Fig. 4. Effects of NEM, ADP, CsA, BKA, CATR, NADH, and Ca^{2+} on Tl^{+}-induced swelling of succinate-energized rat liver mitochondria in the presence of ADP. Mitochondria (1.5 mg/ml of protein) were added to medium like one of Fig. 2. Additions before mitochondria are indicated to right of traces: free of additions (none Ca^{2+}, in bold), 500 μM ADP (ADP), 1 μM CsA (CsA), 6 μM CATR (CATR), and 7 μM BKA (BKA). Numbers on the right of the traces show addition (μM), injected before mitochondria, of NEM (panels A and B) in the medium. Additions of mitochondria (RLM) and 100 μM Ca^{2+} (Ca^{2+}) are shown by arrows. Typical traces from one of three different mitochondrial preparations are presented.

3. Results

3.1. Effects of PAO, tBHP, DIDS, NEM, ADP, CsA, BKA, and CATR on swelling of rat liver mitochondria in the medium containing Tl^{+} and Ca^{2+}

The study of isolated mitochondria in media containing KNO_3 and $TlNO_3$ permits the investigation of how K^{+} and Tl^{+} pass through the IMM, which is easily permeable to NO_3^{-} (Brierley et al., 1970; Saris et al., 1981; Korotkov, 2009). Succinate-energized rat liver mitochondria in nitrate media free of additions showed weak swelling in the media containing KNO_3 alone (Fig. 1A and C) or $TlNO_3$ and KNO_3 (Figs. 1B and D, 2–4). Visible swelling of the mitochondria occurred in the medium containing KNO_3 and 10–20 μM PAO (Fig. 1A and see Table 1 in Korotkov (2016)). Swelling (similar change in A_{540}) was already detected in the medium containing $TlNO_3$, KNO_3, and 2–5 μM PAO, and it was maximized at 20 μM PAO (Fig. 1B and see Table 1 in Korotkov (2016)). Energized mitochondria in the KNO_3 medium did not swell in the presence of 50–500 μM tBHP (Fig. 1C). Swelling of the succinate-energized mitochondria in the $TlNO_3$ medium increased in experiments with 50–75 μM tBHP (Fig. 1D) and was maximal at 100–500 μM tBHP. Injection of 100 μM Ca^{2+} in the medium containing $TlNO_3$, KNO_3, succinate, and rotenone (Fig. 2A, control trace) resulted

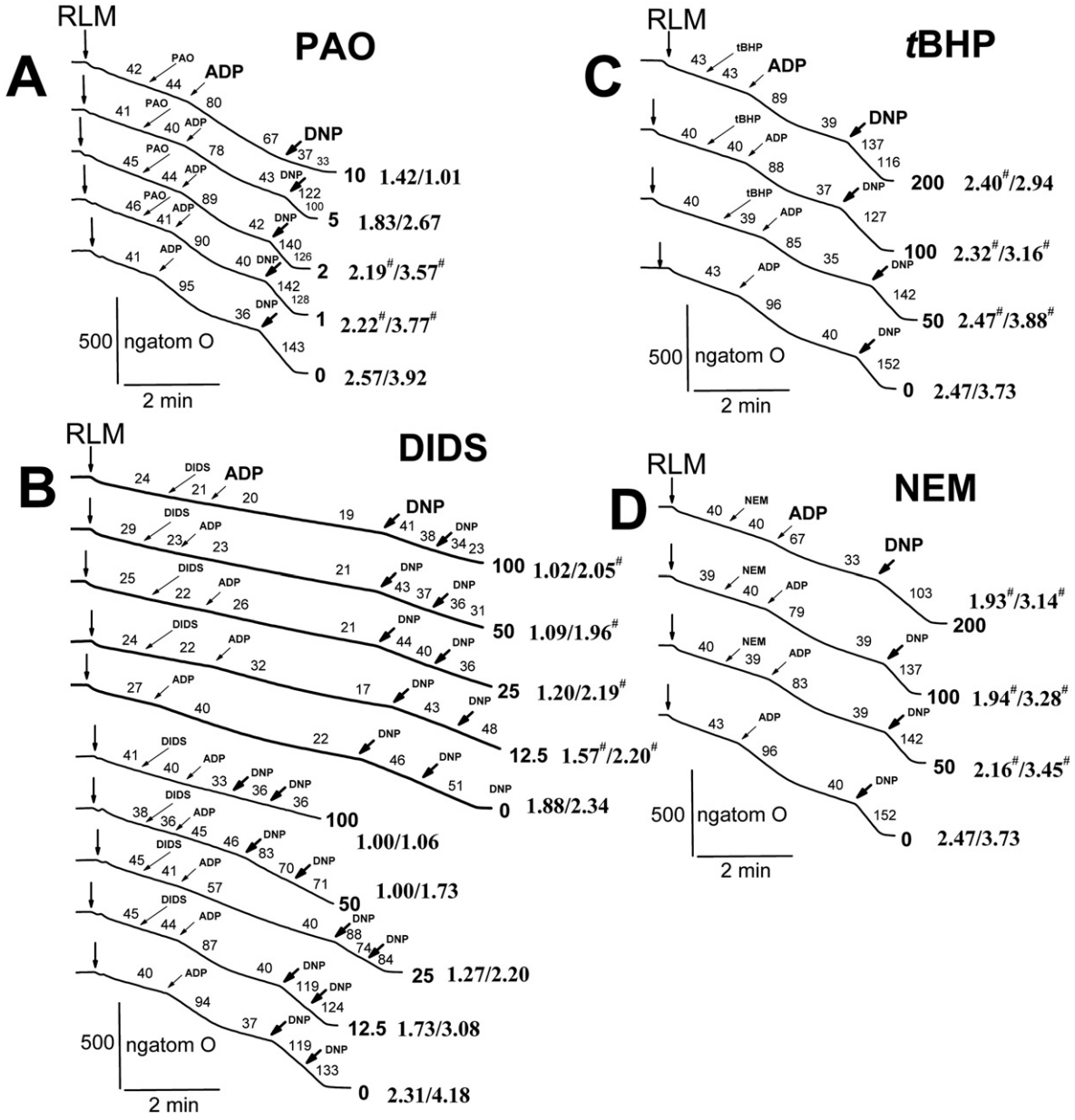

Fig. 5. Influence of PAO, DIDS, tBHP, and NEM on oxygen consumption rates of rat liver mitochondria. Mitochondria (1.5 mg/ml of protein) were added in medium containing 25 mM $TlNO_3$, 100 mM sucrose, 125 mM KNO_3, 5 mM Tris-NO_3 (pH 7.3), 3 mM Tris-P_i, and 3 mM $Mg(NO_3)_2$ as well as 5 mM glutamate and 5 mM malate (panel B, bold traces) or 5 mM succinate and 2 μM rotenone. Additions of mitochondria (RLM), 130 μM ADP (ADP), and 30 μM DNP (DNP) are correspondingly showed by vertical arrows, inclined arrows, and inclined bold arrows. Injections of PAO, DIDS, tBHP, and NEM are correspondingly showed by inclined long arrows (panels A–D). Oxygen consumption rates (ng atom O min/mg of protein) are presented as numbers placed above experimental traces. The numbers on the right of the traces show concentrations (μM): PAO (panel A), DIDS (panel B), tBHP (panel C), and NEM (panel D). Numbers with the slash between them on the right of the traces respectively show values of the RCR_{ADP} and the RCR_{DNP} (see Materials and methods, and more detail Korotkov (2016)). Hash on the right of latter numbers indicates that difference between appropriate values of the RCR_{ADP} and the RCR_{DNP} is statistically insignificant to the values found in experiments free of additions (PAO, tBHP, DIDS, NEM). The rates' deviation (Figs. 5 and 6) was within 5% ($p < 0.05$). Representative traces from one of three independent experiments are presented.

in massive mitochondrial swelling which was additionally accelerated in the presence of 1–10 μM PAO (Fig. 2A). Visible inhibition of the swelling by ADP was found in experiments with 0–2 μM PAO (Fig. 2A and see Table 2 in Korotkov (2016)). The inhibiting effect of ADP some decreased in the presence of 2 μM PAO, and this effect vanished completely at 5–10 μM PAO (Fig. 2A). DIDS at 5–100 μM markedly accelerated the swelling of energized RLM, added into the medium fee of Ca^{2+} (Fig. 2B and see Table 2 in Korotkov (2016)). These mitochondria did not swell in the presence of ADP and 0–5 μM DIDS (Fig. 2B). When ADP was injected into the medium containing $TlNO_3$ and 12.5–50 μM DIDS (Fig. 2B), it inhibited the DIDS-accelerated swelling of succinate-energized RLM. However, inhibiting with ADP was minimal at 100 μM DIDS (Fig. 2B and see Table 2 in Korotkov (2016)). DIDS at 2.5–5 μM did not affect the swelling of CaRLM but some increase in this one was found at 12.5 μM DIDS (Fig. 2C and see Table 2 in Korotkov (2016)). This DIDS-accelerated swelling of CaRLM was inhibited entirely or partially in experiments with ADP and 2.5 μM or 5 μM of DIDS, respectively (Fig. 2C and see Table 2 in Korotkov (2016)). The swelling of energized CaRLM was some accelerated in first minute after injection of Ca^{2+} into the medium containing 50–500 μM tBHP (Fig. 2D). However, this swelling was accordingly inhibited by ADP completely at 25 μM tBHP or partly at 50 μM tBHP (Fig. 2E and see Table 2 in Korotkov (2016)). The swelling of CaRLM was not inhibited by ADP in the presence of 100 and 500 μM tBHP (Fig. 2E and see Table 2 in Korotkov (2016)).

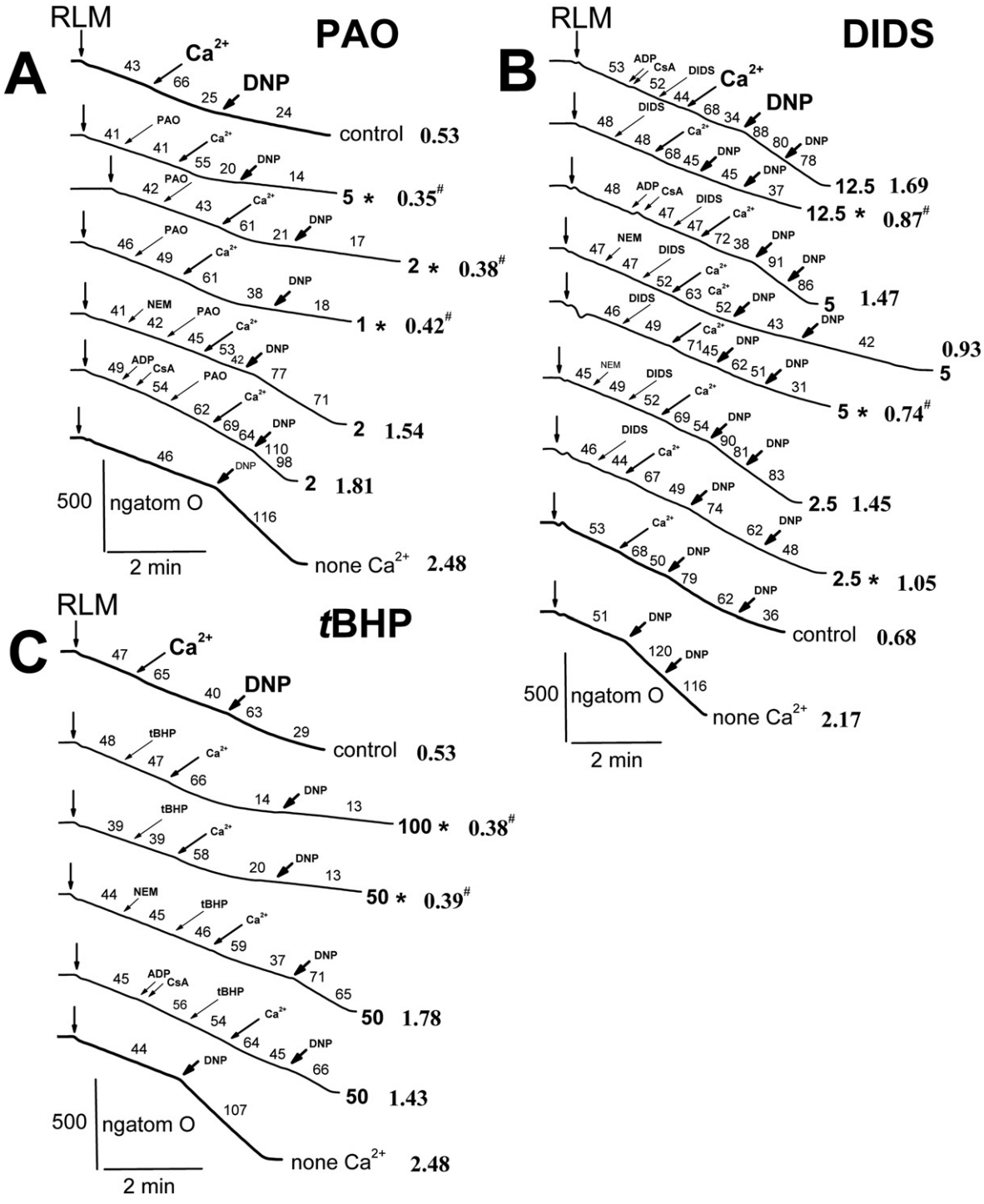

Fig. 6. Influence of PAO, DIDS, tBHP, and Ca^{2+} on oxygen consumption rates of rat liver mitochondria. Mitochondria (1.5 mg/ml of protein) were added in medium containing 75 mM $TlNO_3$, 125 mM KNO_3, 5 mM Tris-NO_3 (pH 7.3), 5 mM succinate, 2 μM rotenone, and 1 μg/ml of oligomycin. Additions of mitochondria (RLM), 100 μM Ca^{2+} (Ca^{2+}), and 30 μM DNP (DNP) are correspondingly showed by vertical arrows, inclined long bold arrows, and inclined bold arrows. Injections of PAO, DIDS, and tBHP are correspondingly showed by inclined long arrows (panels A–C). Additions of 500 μM ADP (ADP), 1 μM CsA (CsA), and 50 μM NEM (NEM) are correspondingly showed by inclined long arrows (panels A–C). Experiments free of additions are indicated on the right of the traces: none Ca^{2+} (free of additions, in bold) and 100 μM Ca^{2+} (control, in bold). The numbers on the right of the traces show concentrations (μM): PAO (panel A), DIDS (panel B), and tBHP (panel C). The asterisks on the right of the traces indicate experiments free of the MPTP inhibitors (ADP, CsA, and NEM). Numbers on the right of the traces in Time New Roman bold show value of the RCR_{DNP} (see Materials and methods, and more detail Korotkov (2016)). Hash on the right of latter numbers indicates that the difference between appropriate value of the RCR_{DNP} is non-relevant statistically to the values found in the control. Oxygen consumption rates (ng atom O min/mg of protein) are presented as numbers placed above experimental traces. Representative traces from one of three independent experiments are presented.

Fig. 3A illustrates that ADP or NEM, but not CsA, markedly inhibited the Ca^{2+}-induced mitochondrial swelling, accelerated by 2 μM PAO. However, the swelling was visibly inhibited in the presence of their binary combinations (Fig. 3A and see Table 3 in Korotkov (2016)), the maximal effects occurring with their mixture (ADP + CsA + NEM). The Ca^{2+}-induced swelling, accelerated by 5 μM DIDS, was partly reduced by ADP alone or CsA plus NEM (Fig. 3B and see Table 3 in Korotkov (2016)) but not by CsA or NEM alone. Maximal inhibition of the swelling was seen in the presence of both ADP plus NEM with/without CsA, and especially in experiments with ADP plus CsA (Fig. 3B and

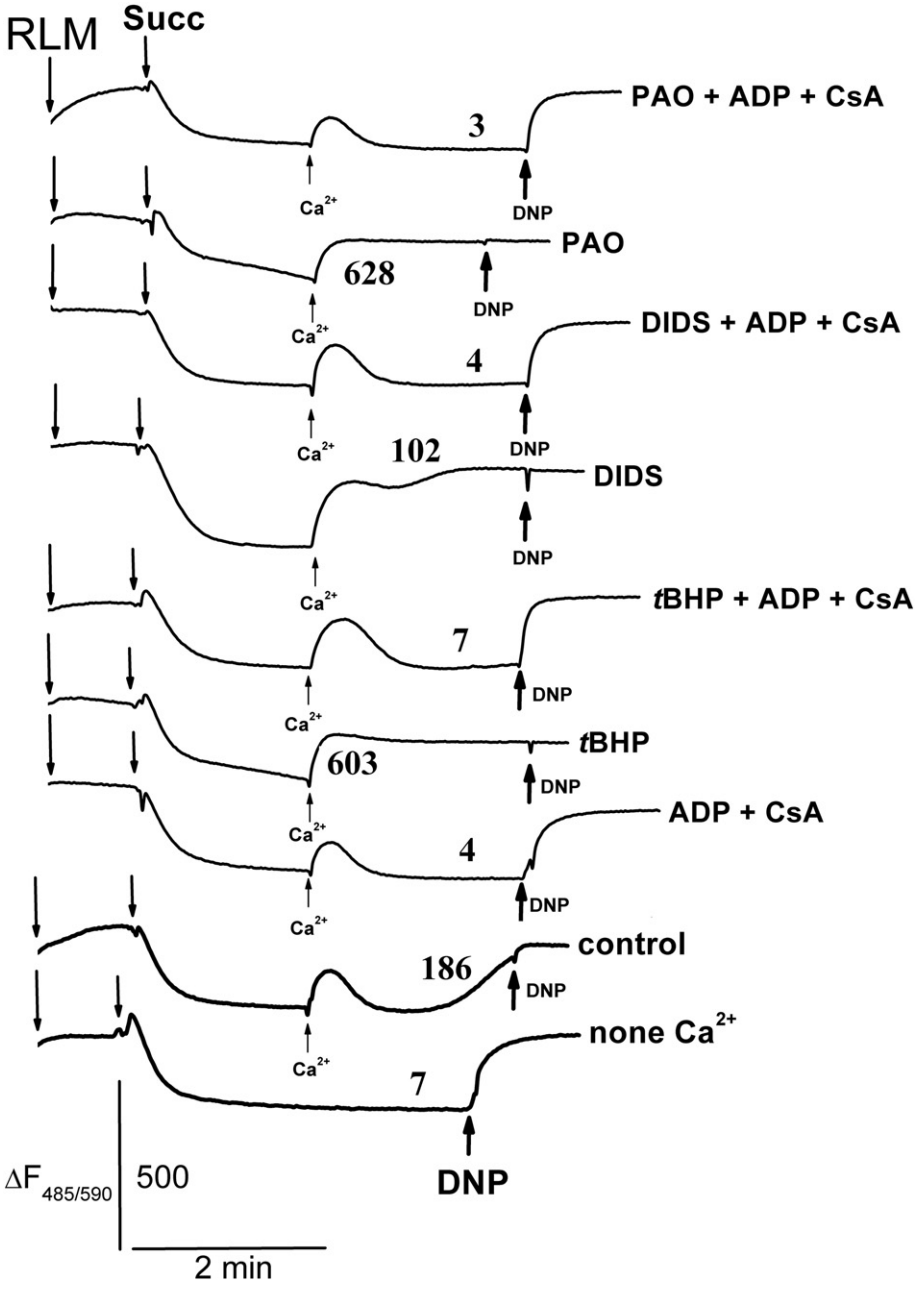

Fig. 7. Effects of PAO, DIDS, tBHP, and Ca^{2+} on the inner membrane potential ($\Delta\Psi_{mito}$) of rat liver mitochondria in the nitrate medium. Mitochondria (0.5 mg/ml of protein) were added to medium containing 20 mM $TlNO_3$, 125 mM KNO_3, 110 mM sucrose, 5 mM Tris-NO_3 (pH 7.3), 1 mM Tris-P_i, 3 μM safranin, 2 μM rotenone, and 1 μg/ml of oligomycin. Additions of mitochondria (RLM) and 5 mM succinate (Succ) are shown by arrows. Following injections of 75 μM Ca^{2+} and 20 μM DNP are correspondingly marked by up-directed arrows and up-directed bold arrows. Experiments free of additions are indicated on the right of the traces: none Ca^{2+} (free of additions, in bold) and 100 μM Ca^{2+} (control, in bold). The rates of $\Delta\Psi_{mito}$ dissipation (arbitrary units per min) are shown as Times New Roman bold numbers placed near experimental traces (more detailed statistics see Korotkov (2016)). Additions before mitochondria are indicated on the right of the traces: 1 μM PAO (PAO), 2.5 μM DIDS (DIDS), 50 μM tBHP, 500 μM ADP (ADP), and 1 μM CsA (CsA). The apparent absorbance change was within 8% ($p < 0.01$). Representative traces from one of three independent experiments are presented.

see Table 3 in Korotkov (2016)). Fig. 3C shows that the Ca^{2+}-induced swelling, accelerated by 50 μM tBHP, was decreased in a lot of CsA > control > NEM, CsA + NEM > ADP > or ADP + NEM > ADP + CsA, ADP + CsA + NEM (see Table 3 in Korotkov (2016), as well). NEM at 50–500 μM enhanced the swelling of succinate-energized RLM after some lag (Fig. 4A and see Table 4 in Korotkov (2016)). NEM at 50 μM decreased the swelling of CaRLM, and reduced ADP inhibition of the swelling with some lag (Fig. 4B and see Table 4 in Korotkov (2016)). The Ca^{2+}-induced swelling increased visibly at 250–500 μM NEM regardless of the presence of ADP (Fig. 4B and see Table 4 in Korotkov (2016)). The swelling of RLM after injection of Ca^{2+} into the medium containing $TlNO_3$ and KNO_3 was decreased in the order of control, CATR > CsA ≫ ADP + CATR > BKA > ADP (Fig. 4C and see Table 4 in Korotkov (2016)).

3.2. Influence of PAO, tBHP, DIDS, NEM, ADP, and CsA on oxygen consumption rates of rat liver mitochondria in the medium containing Tl^+ and Ca^{2+}

Fig. 5 demonstrates the influence of used sulfhydryl reagents (PAO, tBHP, and DIDS) on the oxygen consumption rates of succinate-energized rat liver mitochondria added to 400 mOsm medium containing 25 mM $TlNO_3$ and KNO_3. PAO up to 1–2 μM did not affect markedly both RCR_{DNP} and respiration of the mitochondria being in state 4, state 3, or DNP-uncoupled state but some decrease in RCR_{ADP} had place

(Fig. 5A and see Table 5 in Korotkov (2016)). Wherein, PAO at 5 μM decreased DNP-uncoupled respiration, RCR_{ADP} and RCR_{DNP}, and these three parameters were visibly inhibited by 10 μM PAO. State 4 of RLM, injected into the medium containing glutamate and malate (in bold) or succinate and rotenone, was not affected by 12.5–100 μM DIDS (Fig. 5B). DIDS at 25–100 μM did inhibit state 3 and RCR_{ADP} in Ca^{2+}-free experiments with these substrates, although DNP-uncoupled respiration and RCR_{DNP} were visibly decreased by DIDS only in the succinate-energized mitochondria (Fig. 5B and see Table 5 in Korotkov (2016)). Mitochondrial respiration as well as RCR_{ADP} and RCR_{DNP} were not influenced in the presence of 50–200 μM tBHP, except for a slight decrease in DNP-uncoupled respiration and RCR_{DNP} at 100–200 μM (Fig. 5C and see Table 5 in Korotkov (2016)). NEM at 50–200 μM had no effect on state 4, but somewhat decrease in RCR_{ADP}, RCR_{DNP} as well as state 3 and DNP-uncoupled respiration was found in the presence of these NEM concentrations (Fig. 5D and see Table 5 in Korotkov (2016)). Fig. 6 illustrates that basal respiration, after some short-term burst from Ca^{2+} uptake, and DNP-uncoupled respiration (control trace) compared to the respiration free of any additions (none Ca^{2+} trace) were both decreased after addition of Ca^{2+} in the medium containing $TlNO_3$ and KNO_3. Some Ca^{2+}-induced decrease in DNP-uncoupled respiration (asterisk-marked traces) was found in the presence of 1–5 μM PAO (Fig. 6A) or 50–100 μM tBHP (Fig. 6C) but not 2.5–12.5 μM DIDS (Fig. 6B). However, notable decrease in RCR_{DNP} was detected only at 5 μM PAO (Fig. 6A and see Table 6 in Korotkov (2016)). ADP plus CsA or NEM alone, injected before these reagents (PAO, DIDS, or tBHP), prevented this Ca^{2+}-induced decrease in both DNP-uncoupled respiration and RCR_{DNP} (Fig. 6 and see Table 6 in Korotkov (2016)).

3.3. Influence of PAO, tBHP, DIDS, ADP, and CsA on $\Delta\Psi_{mito}$ dissipation of succinate-energized rat liver mitochondria in the medium containing Tl^+ and Ca^{2+}

Non-Ca^{2+} trace on Fig. 7 shows $\Delta\Psi_{mito}$-driven safranine uptake of succinate-energized RLM, added to the medium containing 20 mM $TlNO_3$ and KNO_3. The drop in the $\Delta\Psi_{mito}$ for some traces immediately after Ca^{2+} administration resulted in the potentially-dependent uptake of Ca^{2+} by these mitochondria. Somewhat Ca^{2+}-induced drop (Fig. 7) in the $\Delta\Psi_{mito}$ (control trace) had place due to the opening of the Tl^+-induced MPTP in the inner membrane of CaRLM (Korotkov and Saris, 2011; Korotkov et al., 2015a, and present study). The Ca^{2+}-induced $\Delta\Psi_{mito}$ drop and corresponding rate in the change of safranine signal were more visible in the presence of PAO, DIDS, or tBHP (Fig. 7 and see Table 7 in Korotkov (2016)). However, these drop and rate were very low when the reagents (PAO, DIDS, or tBHP) were injected in the medium containing ADP plus CsA (Fig. 7 and see Table 7 in Korotkov (2016)).

4. Discussion

It was earlier postulated that MPTP opening in the IMM is induced by the oxidation and cross-linkage of membrane protein thiol groups or respiratory chain-generated ROS (Bernardes et al., 1994; Petronilli et al., 1994; Kowaltowski et al., 1997). Indeed, oxidative stress inductors (diamide and tBHP) and thiol reagent (PAO) were found to cross-link Cys_{159} and Cys_{256} on matrix-facing loops of the ANT, and to induce the MPTP by inhibiting ADP binding and increasing Cyp-D binding with specific sites of the translocase (Petronilli et al., 1994; McStay et al., 2002; Halestrap and Brenner, 2003; García et al., 2007). The sensitivity of the calcium trigger sites to Ca^{2+} increased potently when the ANT 'c' conformation was stabilized by calcium overload, CATR, PAO, tBHP, or diamide (Castilho et al., 1996; McStay et al., 2002; Halestrap and Brenner, 2003; Klingenberg, 2008; Halestrap, 2010). Caused by tBHP or PAO in succinate-energized CaRLM, a diminution in FCCP-uncoupled respiration and an increase in swelling and $\Delta\Psi_{mito}$ dissipation were markedly inhibited by EGTA in the presence of ADP, DTT, catalase, or ruthenium red (Riley and Pfeiffer, 1985; Castilho et al., 1996; Kowaltowski and Castilho, 1997). The Ca^{2+}- and FCCP-induced MPTP, the affinity of ADP to its inhibitory site, and the subsequent swelling of RLM in a KCl buffer increased in series of tBHP, diamide < PAO (Halestrap et al., 1997). The ability of the thiol reagents (PAO, tBHP, DIDS) to overcome the ADP inhibition of the Tl^+-induced MPTP in CaRLM enhances in the series of tBHP < DIDS < PAO because the reagents' concentration to cause similar effects on swelling (Fig. 2 and see Table 2 in Korotkov (2016)), respiration (Figs. 5 and 6, and see Tables 5 and 6 in Korotkov (2016)), and $\Delta\Psi_{mito}$ (Fig. 7 and see Table 7 in Korotkov (2016)) was similarly decreased in experiments with Ca^{2+} and ADP. The MPTP inhibitor, ADP fixing the ANT 'm' conformation decreased sensitivity of calcium trigger sites to Ca^{2+} (Halestrap and Brenner, 2003; Klingenberg, 2008; Halestrap, 2010). The present research reveals that Ca^{2+}-induced increase in the swelling (Fig. 2 and see Table 2 in Korotkov (2016)) and $\Delta\Psi_{mito}$ dissipation (Fig. 7 and see Table 7 in Korotkov (2016)) as well as attenuation in DNP-uncoupled respiration (Fig. 6 and see Table 6 in Korotkov (2016)) were visibly inhibited by ADP. Taking into account these results and above-mentioned literature data, we can hypothesize carefully that opening of the Tl^+-induced MPTP in the inner membrane can be dependent on the ANT conformation state.

It was earlier shown that BKA and CATR, respectively, fix ANT in 'm' and 'c' conformation, transforming the mitochondria into condensed and non-condensed state (Halestrap and Brenner, 2003; Klingenberg, 2008; Halestrap, 2010). Ca^{2+}, P_i-induced MPTP was stimulated by CATR but inhibited by Mg^{2+}, ADP, and BKA (Zoccarato et al., 1981). The finding that the ADP-dependent decrease in Ca^{2+}-induced swelling of CaRLM was overcome by CATR (Fig. 4C and see Table 4 in Korotkov (2016)) is in a good agreement with the fact that MPTP opening took place when the ANT in Ca^{2+}-loaded mitochondria was in 'c' conformation (Klingenberg, 2008; Halestrap, 2010). On the other hand, the inhibition in swelling of CaRLM in experiments with ADP or BKA (Fig. 4C) can be resulted in fixing the ANT 'm' conformation by these agents (Halestrap and Brenner, 2003; Halestrap, 2010). Low concentrations of NEM were found to attack Cys_{56} that stabilizes the ANT in 'm' conformation (Halestrap and Brenner, 2003; Nantes et al., 2011). As a result, NEM in experiments with thiol reagents (tBHP, diamide, arsenite, menadione, DIDS, and PAO) inhibited Ca^{2+}-induced MPTP, mitochondrial swelling, $\Delta\Psi_{mito}$ dissipation due to a decrease in the affinity of calcium-binding sites to Ca^{2+} (Petronilli et al., 1994; Kowaltowski et al., 1997; McStay et al., 2002; Halestrap and Brenner, 2003; García et al., 2007; Nantes et al., 2011). Thus, a decrease of the Ca^{2+}-induced swelling, caused by NEM, in the presence of PAO and tBHP (Fig. 3 and see Table 3 in Korotkov (2016)) may be due to fixing the ANT in 'm' conformation. The impact of MPTP inducers (PAO, tBHP, and DIDS) on the total thiol content in mitochondrial proteins was additive (Kowaltowski et al., 1997). This suggests that the inducers may react with distinct thiol groups of mitochondrial membrane proteins. Possibly for this reason, the attenuation of Ca^{2+}-induced mitochondrial swelling caused by NEM was not significant in experiments with DIDS (Fig. 3B and see Table 3 in Korotkov (2016)). The amount of membrane protein thiols accessible to NEM increased visibly in the presence of ADP stabilizing the ANT in 'm' conformation (Kowaltowski et al., 1997). It can be assumed that the more stabilizing of the 'm' conformation resulted in a stronger inhibition of the Tl^+-induced MPTP opening in the joint presence of ADP and NEM that was correspondingly manifested as attenuation of Ca^{2+}-induced swelling (Fig. 3 and see Table 3 in Korotkov (2016)) and the inhibition in decrease of DNP-uncoupled respiration (Fig. 6 and see Table 3 in Korotkov (2016)) in experiments with PAO, tBHP, and DIDS.

It was shown that CsA prevented the binding of Cyp-D to the matrix surface and inhibited the opening of MPTP in the IMM (Halestrap and Brenner, 2003; Halestrap, 2010). Induced by oxidative stress inducers (PAO, tBHP, diamide, DIDS, Cd^{2+}), swelling, $\Delta\Psi_{mito}$ disruption, Ca^{2+} efflux, and increased CyP-D binding were inhibited by CsA (Bernardes

et al., 1994; Broekemeier and Pfeiffer, 1995; Kowaltowski and Castilho, 1997; Zazueta et al., 2000; McStay et al., 2002; Halestrap and Brenner, 2003; Belyaeva et al., 2004; García et al., 2007). Earlier we found (Korotkov and Saris, 2011; Korotkov et al., 2015b) that increase in swelling or $\Delta\Psi_{mito}$ drop and decrease in mitochondrial respiration were followed by the Tl^+-induced MPTP opening in the inner membrane of CaRLM, added to medium containing 25–75 mM $TlNO_3$ and 25–100 μM Ca^{2+} as well as sucrose or nitrates. Inhibition of the MPTP was observed in experiments with CsA and ADP, and this inhibition increased in series of CsA < ADP ≪ ADP + CsA (Korotkov and Saris, 2011; Korotkov et al., 2015b). Similar series were seen under inhibiting the increased swelling (Fig. 3 and see Table 3 in Korotkov (2016)), respiratory decrease (Fig. 6 and see Table 6 in Korotkov (2016)), and Ca^{2+}-induced $\Delta\Psi_{mito}$ dissipation (Fig. 7 and see Table 7 in Korotkov (2016)) in our experiments with PAO, tBHP and DIDS. The replacement of ADP by NEM in the presence of CsA maintained the series (Figs. 3 and 6 as well as Tables 3 and 6 in Korotkov (2016)). The results suggest that the additive effect in experiments with CsA is possible if the ANT 'm' conformation is stabilized by both ADP and NEM (Halestrap and Brenner, 2003; Halestrap, 2010; Nantes et al., 2011). However, the inhibition of the Ca^{2+}-induced swelling by CsA plus NEM was not so significant in experiments with DIDS (Fig. 3B and see Table 3 in Korotkov (2016)), and it was comparable to the effect of ADP alone, but not ADP plus CsA. This difference may be due to the fact that PAO and tBHP, on the one hand, and DIDS, on the other hand, may react with different mitochondrial membrane protein thiol groups (Kowaltowski et al., 1997) and induce distinct sulfhydryl–disulfide transitions, followed by membrane protein polymerization in the presence of Ca^{2+} (Bernardes et al., 1994).

It was found that titration of approximately 11 nmol/mg protein of mitochondrial thiol groups is required to open the MPTP and to induce massive swelling of mitochondria (Riley and Lehninger, 1964; Brierley et al., 1968; García et al., 2007). Thiol reagents (PAO, tBHP, DIDS, and 100–200 μM NEM) stabilize the pore structure via cross-linkage of vicinal matrix-faced dithiol sites of proteins involved in the formation of the pore which was shown to be dependent on extra-mitochondrial Ca^{2+} that triggers membrane permeabilization with associated mitochondrial swelling, reduction in mitochondrial electron flow and thiol content, $\Delta\Psi_{mito}$ dissipation, oxidation of pyridine nucleotides, and significant enhancement of ROS production, as well as the formation of mitochondrial protein aggregates and release of Ca^{2+}, Mg^{2+}, and K^+ from the matrix (Riley and Pfeiffer, 1985; Bernardes et al., 1994; Broekemeier and Pfeiffer, 1995; Rigobello et al., 1995; Castilho et al., 1996; Bindoli et al., 1997; Kowaltowski et al., 1997; Nantes et al., 2011; Singh et al., 2011). EGTA inhibited both mitochondrial swelling and $\Delta\Psi_{mito}$ drop, and decreased the amount of protein aggregates in experiments with DIDS and Ca^{2+} (Bernardes et al., 1994). On the other hand, the harmful effect of Tl^+ on living organisms was presumed to be resulted in ligand formation with protein sulfhydryl groups (Woods and Fowler, 1986; Mulkey and Oehme, 1993; Kiliç and Kutlu, 2010). We have recently suggested formation of complexes of Tl^+ with soluble matrix proteins because a decrease in the content of the SH groups was found in the matrix-soluble fraction of RLM, incubated and frozen in the medium containing 25–75 mM $TlNO_3$ and KNO_3 (Korotkov et al., 2014a). Thereby, the increase (Figs. 1–7 and see Tables 1–7 in Korotkov (2016)) in effects of Tl^+ on RLM, added in media containing $TlNO_3$, KNO_3, and used sulfhydryl reagents (PAO, tBHP, DIDS), appears to be due to a magnification in forming these thallous complexes. As can be surmised, the substantial swelling after addition of Ca^{2+} into the medium containing the thiols (PAO, tBHP, DIDS) (Fig. 2 and see Table 2 in Korotkov (2016)) might be due to increased membrane permeabilization resulting from the aggregation of mitochondrial proteins with Tl^+. The present study is the first to show (Figs. 1 and 2) that the ability of rat liver mitochondria to maintain stability of their matrix volume in $TlNO_3$ media (Korotkov, 2009) depends on reactivity of thiol groups in the inner membrane and markedly decreases in the presence of these reagents.

Experiments in which mitochondria were pre-treated with diamide and PAO revealed the interaction of 80 μM EMA or 500 μM NEM with the ANT Cys_{159} which greatly lowered the ability of ADP to inhibit the MPTP (McStay et al., 2002). The Cd^{2+}-induced MPTP opening increased in the presence of NEM, since Cd^{2+} (unlike the thiols used by us) forms an adduct with the vicinal Cys_{56} and Cys_{159} rather than Cys_{159} and Cys_{256} of the ANT (Zazueta et al., 2000; Belyaeva et al., 2004). DTT reduced vicinal SH groups which had been preliminarily oxidized by Cd^{2+} and the cross-linkers (tBHP or diamide) or bridged with arsenite (Petronilli et al., 1994; Zazueta et al., 2000). Changes in the ANT conformation may be involved in the changeover of thiol group reactivity (Kowaltowski et al., 1997; McStay et al., 2002). So, one can assume that the visible increase in the swelling of succinate-energized RLM at 500 μM NEM (Fig. 4A and see Table 4 in Korotkov (2016)) and elimination of the ADP inhibition of Ca^{2+}-induced swelling at 250–500 μM NEM (Fig. 4B) may result from the change of the ANT conformation resulted in interaction of NEM with the ANT thiol groups.

It was found that tBHP in media free of Ca^{2+} induced membrane permeabilization via oxidation or cross-linkage of vicinal thiol groups, and increased the mitochondrial swelling and $\Delta\Psi_{mito}$ drop, as well as oxidization of pyridine nucleotides, glutathione, and NADH (Bindoli et al., 1997; Salvi et al., 2007; Singh et al., 2011). The mitochondrial permeabilization induced by the thiol reactant DIDS was mediated by its interaction with membrane proteins (Nantes et al., 2011). It was earlier presumed that membrane permeabilization to ions does not require extensive thiol cross-linkage, and may occur even with modification of single proteins via sulfhydryl–disulfide transitions in bond formation (Bernardes et al., 1994; Castilho et al., 1996). It is known that a dysfunction of the respiratory chain favors MPTP opening (Chávez et al., 1997). A decrease in DNP-uncoupled respiration and RCR_{DNP} (Fig. 5 and see Table 5 in Korotkov (2016)) in experiments with the thiol reagents (PAO, tBHP, and DIDS) or Cd^{2+} (Korotkov et al., 1998) indicates inhibition of the respiratory chain under our used experimental conditions. One may therefore carefully suppose that more potent swelling of succinate-energized RLM in the medium containing $TlNO_3$ and KNO_3 as well as PAO and tBHP (Fig. 1 and see Table 1 in Korotkov (2016)) or DIDS (Fig. 2B and see Table 2 in Korotkov (2016)) is most likely due to inhibition of the respiratory chain by these reagents, but not to increased inner membrane passive ion permeability. On the other hand, ANT can be transformed from an antiporter to a non-selective porter by increasing CyP-D binding with the IMM (Li et al., 2004). The inhibition of swelling in a medium containing ADP and NH_4NO_3 allows the penetration of H^+ and K^+ into the matrix to be assumed with the ANT participation (Klingenberg, 2008). The swelling of non-energized RLM in $TlNO_3$ media free of Ca^{2+} was decreased by ADP in our experiments with Y^{3+} and La^{3+} (Korotkov et al., 2014b) or Tl^+ alone (Korotkov and Saris, 2011), possibly indicating that ANT participates in regulating inner membrane ion permeability. Thus, a second reason for the swelling may be the reaction of the thiol reagents with SH groups of the ANT (Petronilli et al., 2009; Nantes et al., 2011; Ricchelli et al., 2011). The reason for the PAO-induced decrease (Fig. 1A and see Table 1 in Korotkov (2016)) and tBHP-induced lack (Fig. 1C) in swelling of RLM in the KNO_3 medium may be that Tl^+ more than K^+ favors interaction of the reagents with the ANT in medium containing $TlNO_3$ and KNO_3. When DIDS at 50–100 μM has interacted with thiol groups, it has correspondingly decreased FCCP-uncoupled respiration in succinate-energized RLM and state 3 in α-ketoglutarate-energized RLM due to the inhibition of succinate dehydrogenase activity and F_1F_0-ATP synthase (Bernardes et al., 1994; Bernardes et al., 1997). DIDS completely inhibited RCR_{ADP} and state 3 respiration of RLM, regardless of the substrate used (Fig. 5B and see Table 5 in Korotkov (2016)), however DNP-uncoupled respiration was completely inhibited by 100 μM DIDS only in succinate-energized mitochondria that is in a good agree with previous findings (Bernardes et al., 1994; Bernardes et al., 1997).

It was found that hepatocytes, cardiomyocytes, renal tubular epithelial cells, glial cells, and neurons in thallium-empoisoned humans

(Rodríguez-Mercado and Altamirano-Lozano, 2013; Li et al., 2015), as well as thallium-treated rodents (Herman and Bensch, 1967; Woods and Fowler, 1986; Leung and Ooi, 2000; Kiliç and Kutlu, 2010) showed significant disruption of the structural integrity of mitochondria which manifested in intense mitochondrial swelling, notable expansion of intermembrane spaces, and disintegration of membranes and cristae. Dose of thallous salts both above cases and thallium-treated hamsters (Aoyama et al., 1988) was approximately to 120–900 μmoles Tl^+ per l of body water. Thallous salts at 100–250 μM were used in experiments with isolated rat hepatocytes and PC12 cells as well as long-term incubated RLM (Zierold, 2000; Villaverde et al., 2004; Hanzel and Verstraeten, 2006; Hanzel and Verstraeten, 2009; Pourahmad et al., 2010; Eskandari et al., 2015). Concentration at 2–150 mM thallium salt was used in researching oxygen consumption rates and potassium ion fluxes in isolated mitochondria (Barrera and Gomez-Puyou, 1975; Melnick et al., 1976; Diwan and Lehrer, 1977; Korotkov et al., 2008; Wojtovich et al., 2010) as well as potassium channels of both frog oocytes (Lopatin et al., 1998; Lu et al., 2001) and ventricular myocytes (Foster et al., 2012), and renal proximal tubule membrane (Mauerer et al., 1998). Visible mitochondrial swelling could be detected only if isolated mitochondria were injected into millimolar thallous buffers (Melnick et al., 1976; Saris et al., 1981; Korotkov, 2009; Korotkov et al., 2015b). The reason for this can be in part that Tl^+ revealed negligible interaction with inner membrane sulfhydryl groups of RLM because a change in the content of the SH groups was not found in the inner membrane fraction of RLM, exposed in the medium containing 25–75 mM $TlNO_3$ and further washed and frozen in the medium containing 125 mM KNO_3 (Korotkov et al., 2014a). Therewith thallous salts at millimolar concentrations pure reacted with both mitochondrial respiratory enzymes (Melnick et al., 1976; Woods and Fowler, 1986; Mulkey and Oehme, 1993; Korotkov, 2009) and molecules possessing vicinal SH groups (Perrin, 1979). On the other hand, chelating agents (dimercaptopropanol, ethylenediaminetetraacetic acid, diethyldithiocarbamate) used against bivalent heavy metals' toxicity are contraindicated in the treatment of thallium poisoning. An optimal therapy for thallium intoxication is the injection of Prussian blue combined with forced diuresis with furosemide and mannitol, which may be supplemented by hemodialysis (Blain and Kazantzis, 2015). The increase of Ca^{2+} concentration in cytoplasm was found in experiments with isolated rat hepatocytes injected into a buffer containing TlCl (Zierold, 2000). Cytotoxic effects of $TlNO_3$ including decrease in $\Delta\Psi_{mito}$ were markedly decreased in isolated rat hepatocytes in the presence of MPTP inhibitors (CsA and carnitine) (Pourahmad et al., 2010). The present study using millimolar $TlNO_3$ concentrations (Figs. 1–7) was earlier performed the in vitro model that we have proposed to study opening of Tl^+-induced MPTP in the inner membrane of Ca^{2+}-loaded rat liver and heart mitochondria (Korotkov and Saris, 2011; Korotkov et al., 2013) and described in detail in our recent manuscript (Korotkov et al., 2015b). Thus, the use of millimolar thallous concentrations and micromolar Cd^{2+} concentrations (Korotkov et al., 1998) proved weak interaction of Tl^+ (Korotkov et al., 2014a) but not Cd^{2+} (Zazueta et al., 2000) with thiol groups of isolated rat liver mitochondria. On the other hand, the research of different order concentrations of Tl^+ in various experimental models showed obvious qualitative similarity in thallous effects.

Thallium is a rare but widely dispersed element and it is more toxic to humans than mercury, cadmium, lead, copper or zinc (Peter and Viraraghavan, 2005; Rodríguez-Mercado and Altamirano-Lozano, 2013). Whereby, symptoms of acute toxicity depend on age, thallium dose, route of administration (Peter and Viraraghavan, 2005). Intake of thallium compounds is very fast after ingestion, inhalation, or skin contact and may be full after ingestion (Blain and Kazantzis, 2015). Thallium oxide of 100–350 μM was very toxic for rats, rabbits and dogs (Schoer, 1984). Levels of thallium bioaccumulation in fish were related to the age and length of the fish, and greater bioaccumulation of inorganic thallium can be possible in water containing low amounts of potassium (Gantner et al., 2009). Thallium concentration in liver of thallium-poisoned martens and badgers was from 4.7 to 57 mg/kg that is equal to Tl^+ at 23–280 μM (Schoer, 1984). Thallium concentration on the first or third day after single injection of Tl acetate in hamsters (50 mg/kg) was correspondingly equal to 1330 μM and 470 μM in kidney, and 180 and 140 μM in liver (Aoyama et al., 1988). Thallium poisoning (Herman and Bensch, 1967; Kiliç and Kutlu, 2010; Li et al., 2015) resulted in appearance of high electron dense granules which were detected in cytoplasm and mitochondria of brain, kidney, and liver. Appearance of these granules can be likely caused by the deposition of thallium in cells of these organs. These granules in hepatocytes of thallium-poisoned rats were similar ones found after calcium overload of mitochondria and hepatocytes (Herman and Bensch, 1967). Therefore we cannot exclude that actual concentrations of Tl^+ in cytoplasm can be considerably higher micromolar concentrations of thallous salts used in experiments with isolated cells and thallium-treated animals. Thallous compounds have been widely used in optical, cement, consume jewelry, photographic and electronic industries as well as they applied as insecticide and rodenticide agents (Peter and Viraraghavan, 2005; Ramsden, 2007; Kiliç and Kutlu, 2010; Blain and Kazantzis, 2015; Li et al., 2015). However, emerging warfarin resistance in rats, the latter use of thallium increased again in some other countries (Peter and Viraraghavan, 2005; Blain and Kazantzis, 2015). Fatalities have also occurred after the now outdated therapeutic use of thallium (Blain and Kazantzis, 2015). Exposure of man to thallium may result in atmospheric pollution from copper, lead, and zinc smelters and from coal-burning power plants, and as a by-product of cadmium production and catalysts in organic synthesis (Blain and Kazantzis, 2015). Thereby, of even greater opening the MPTP (Figs. 1–4, 6, 7 and see Tables 1–4, 6, 7 in Korotkov (2016)) in $TlNO_3$ media containing used thiol reagents (PAO, tBHP, DIDS) allows to carefully suggest that toxic effects of thallous compounds present in the environment can be significantly increased if other sulfhydryl compounds such as industrial oxidizers or compounds of bivalent heavy metals (Pb, Sn, Hg, Cd) and arsenic are present there. On the other hand, the medical use of thallium isotopes (Hsieh et al., 2012) should not be performed simultaneously with other medications reducing antioxidant protection of an organism.

Like bivalent heavy metals, thallium is widely believed to bind with thiol groups of proteins and mitochondrial membranes, and this circumstance results in inhibiting of enzyme reactions and decrease in glutathione levels with increased lipid peroxidation, and as a consequence, cellular injury (Aoyama et al., 1988; Ramsden, 2007; Kiliç and Kutlu, 2010). It was shown that Tl^+ and Tl^{3+} enhanced the production of ROS and H_2O_2, stimulated lipid peroxidation, and decreased the intracellular and matrix glutathione in experiments with PC12 cells, isolated hepatocytes, and thallium-treated rats, but the biochemical mechanisms of these toxic effects are still unclear (Villaverde et al., 2004; Galván-Arzate et al., 2005; Hanzel and Verstraeten, 2006; Hanzel and Verstraeten, 2009; Kiliç and Kutlu, 2010; Pourahmad et al., 2010). It must be stressed that these above experiments have not revealed any significant differences between the effects of Tl^+ and Tl^{3+} (potent oxidizer) in above experiments with cells and mitochondria (Rodríguez-Mercado and Altamirano-Lozano, 2013). In contrast to the experiments using potent thiol reagents such as 15 μM PAO (Kowaltowski et al., 1997), 5–10 μM Cd^{2+} (Zazueta et al., 2000), or 10–20 μM Ag^+ (Riley and Lehninger, 1964), we have not found any interaction of Tl^+ with SH groups of the inner membrane of RLM, injected in the medium containing 25–50 mM $TlNO_3$ (Korotkov et al., 2014a). These circumstances gave us reason to hypothesize that oxidation of Tl^+ to Tl^{3+} around inner membrane micro-domains may be due to the interaction of Tl^+ with ROS, generated by mitochondrial respiratory chain complexes (Korotkov et al., 2015b). We recently showed (Korotkov et al., 2015c) that the opening of the Tl^+-induced MPTP was more intensive in the presence of diamide but not tBHP because diamide more than tBHP can decrease glutathione level in cells and mitochondria (Petronilli et al., 1994; Halestrap and Brenner, 2003; Halestrap, 2010). It is possible

that glutathione oxidation in the above experiments can be resulted in the reaction of glutathione with both ROS and Tl^{3+} which may again be reduced to Tl^{+}. Furthermore, it cannot be ruled out that the reduction of Tl^{3+} to Tl^{+} may be associated with the formation of disulfide bridges between vicinal protein thiol groups of mitochondrial enzymes, including the ANT. To clarify the glutathione decrease in above experiments, additional studies should be carried out with thallium-treated animals and isolated cells in using thallous buffers.

The K^{+} surrogate Tl^{+} possesses crystal radius similar to one of K^{+} therefore the first toxicity can be partially attributed to interaction of Tl^{+} with (Na^{+}/K^{+})-ATPase and membrane channels and transporters, associated to K^{+} and placed in cellular and inner mitochondrial membranes (Gehring and Hammond, 1967; Schoer, 1984; Aoyama et al., 1988; Mulkey and Oehme, 1993; Galván-Arzate and Santamaría, 1998; Peter and Viraraghavan, 2005; Ramsden, 2007; Wojtovich et al., 2010; Blain and Kazantzis, 2015). To research comprehensively processes of H^{+} and Na^{+} movements via IMM was accordingly proposed swelling technique applied media containing 125–135 mM of NH_4NO_3 or $NaNO_3$ because IMM is freely permeable to NO_3^{-} (Mitchell and Moyle, 1969; Brierley et al., 1977). On the other hand, mitochondria preswollen in media containing 125–135 mM KNO_3 buffers showed a massive contraction only if there were thiol reagents or ionophores (Mitchell and Moyle, 1969; Brierley et al., 1977). Swelling of isolated mitochondria in media containing KCl or mannitol plus sucrose allows to be investigated by the MPTP in low and high conduction state, respectively (Bernardes et al., 1994; Chávez et al., 1997; Halestrap et al., 1997; Kowaltowski and Castilho, 1997; Elustondo et al., 2015). However, swelling in nitrate media can yield information not only on the MPTP low conduction state, but also to research bidirectional movements of univalent cations (H^{+}, K^{+}, and Na^{+}) through the inner membrane (Mitchell and Moyle, 1969; Brierley et al., 1977). Our experiments with swelling of RLM in media containing 25–75 mM $TlNO_3$ plus KNO_3 discovered the Tl^{+}-induced increase in passive ion permeability of IMM, and showed participation of the mitochondrial K^{+}/H^{+} exchanger in extruding the Tl^{+}-induced excess of K^{+}, $H^{+}(NH_4^{+})$, and Na^{+} from the matrix (Korotkov, 2009).

The use of this model allowed us to estimate the involvement calcium sites, directed both external and matrix sides of the inner membrane, in opening of the Tl^{+}-induced MPTP in our experiments with Y^{3+}, La^{3+}, and bivalent metals (Korotkov et al., 2014b). Therewith, it was shown that closure of ATP sensitive (mitoK$_{ATP}$) or BK-type Ca^{2+} activated (mitoK$_{Ca}$) channels triggered the MPTP opening in the inner membrane of CaRLM (Korotkov et al., 2015a). It was found that the Tl^{+}-induced MPTP opening in energized CaRLM was visibly decreased by classic pore inhibitors (ADP, CsA, Mg^{2+}, BKA, and low NEM) and stimulated by classic pore inducers (CATR, high NEM, PAO, tBHP, diamide, and DIDS) (Korotkov and Saris, 2011; Korotkov et al., 2015b; Korotkov et al., 2015c; and present study (Fig. 4C)). Wherein, the application of isolated mitochondria to evaluate mechanisms underlying mitochondrial toxicity of various chemicals and heavy metals is quite justified in place of experiments using animals (Ogata et al., 1983). So, the use of K^{+} surrogate Tl^{+} in the model of the Tl^{+}-induced MPTP at in vitro toxicological studies can help in both studying biochemical mechanisms of thallium toxicity and finding the pore new inhibitors and inducers among different chemical and natural compounds.

The present study results about possible involvement of the ANT conformation in opening the Tl^{+}-induced MPTP that can be some basis for more detailed proteomic studies using isolated mitochondria, cells and Tl-treated animals to ascertain the possible participation of the ANT cysteines (Cys_{159}, Cys_{256}, and Cys_{56}) in both opening and inhibiting of the pore in the inner mitochondrial membrane. Taking into consideration recent findings on the involvement of the mitochondrial phosphate carrier in the MPTP complex (Baines, 2009; Halestrap, 2010), we will focus our efforts on the carrier participation in the Tl-induced MPTP in experiments with CaRLM (in preparation). It must be emphasized that the use of isolated or line cells can confirm the involvement of bioconcentration of Tl^{+} in cytoplasm as well as prove the involvement of the potential mechanisms of toxicity. Although isolated mitochondria enable to get a suitable model for mechanistic studies, they first of all should help us in understanding the thallium toxicity in vivo.

Conflict of interest

No conflicts of interest, financial or otherwise, are declared by the authors.

Transparency Document

The Transparency document associated with this article can be found, in online version.

Acknowledgments

Authors are grateful to Ms. Terttu Kaustia for correcting the English. Purchase of BKA and CATR was financed by a grant from the Russian Foundation for Basic Research to Margarita V. Savina (#08-04-00564a); the funding organization does not have control over the resulting publication Safranin fluorescence was measured using of Research Resource Center equipment for the physiological, biochemical and molecular-biological studies (Sechenov Institute of Evolutionary Physiology and Biochemistry, the Russian Academy of Sciences).

References

Aoyama, H., Yoshida, M., Yamamura, Y., 1988. Induction of lipid peroxidation in tissues of thallous malonate-treated hamster. Toxicology 53, 11–18.
Baines, C.P., 2009. The molecular composition of the mitochondrial permeability transition pore. J. Mol. Cell. Cardiol. 46, 850–857.
Barrera, H., Gomez-Puyou, A., 1975. Characteristics of the movement of K^{+} across the mitochondrial membrane and the inhibitory action of Tl^{+}. J. Biol. Chem. 250, 5370–5374.
Belyaeva, E.A., Glazunov, V.V., Korotkov, S.M., 2004. Cd^{2+} versus Ca^{2+}-produced mitochondrial membrane permeabilization: a proposed direct participation of respiratory complexes I and III. Chem. Biol. Interact. 150, 253–270.
Bernardes, C.F., Meyer-Fernandes, J.R., Basseres, D.S., Castilho, R.F., Vercesi, A.E., 1994. Ca^{2+}-dependent permeabilization of the inner mitochondrial membrane by 4,4′-diisothiocyanatostilbene-2,2′-disulfonic acid (DIDS). Biochim. Biophys. Acta 1188, 93–100.
Bernardes, C.F., Meyer-Fernandes, J.R., Martins, O.B., Vercesi, A.E., 1997. Inhibition of succinic dehydrogenase and F_0F_1-ATP synthase by 4,4′-diisothiocyanatostilbene-2,2′-disulfonic acid (DIDS). Z. Naturforsch. C. 52, 799–806.
Bernardi, P., 2013. The mitochondrial permeability transition pore: a mystery solved? Front. Physiol. 4, 95. http://dx.doi.org/10.3389/fphys.2013.00095.
Bindoli, A., Callegaro, M.T., Barzon, E., Benetti, M., Rigobello, M.P., 1997. Influence of the redox state of pyridine nucleotides on mitochondrial sulfhydryl groups and permeability transition. Arch. Biochem. Biophys. 342, 22–28.
Blain, R., Kazantzis, G., 2015. Thallium. In: Nordberg, G.F., Fowler, B.A., Nordberg, M. (Eds.), Handbook on the Toxicology of MetalsSpecific Metals vol. II. Elsevier, pp. 1229–1240.
Bonora, M., Bononi, A., De Marchi, E., Giorgi, C., Lebiedzinska, M., Marchi, S., Patergnani, S., Rimessi, A., Suski, J.M., Wojtala, A., Wieckowski, M.R., Kroemer, G., Galluzzi, L., Pinton, P., 2013. Role of the c subunit of the F_0 ATP synthase in mitochondrial permeability transition. Cell Cycle 12, 674–683.
Bonora, M., Wieckowski, M.R., Chinopoulos, C., Kepp, O., Kroemer, G., Galluzzi, L., Pinton, P., 2015. Molecular mechanisms of cell death: central implication of ATP synthase in mitochondrial permeability transition. Oncogene 34, 1475–1486.
Brierley, G.P., Knight, V.A., Settlemire, C.T., 1968. Ion transport by heart mitochondria. XII. Activation of monovalent cation uptake by sulfhydrly group reagents. J. Biol. Chem. 243, 5035–5043.
Brierley, G.P., Jurkowitz, M., Scott, K.M., Merola, A.J., 1970. Ion transport by heart mitochondria. XX. Factors affecting passive osmotic swelling of isolated mitochondria. J. Biol. Chem. 245, 5404–5411.
Brierley, G.P., Jurkowitz, M., Chávez, E., Jung, D.W., 1977. Energy-dependent contraction of swollen heart mitochondria. J. Biol. Chem. 252, 7932–7939.
Broekemeier, K.M., Pfeiffer, D.R., 1995. Inhibition of the mitochondrial permeability transition by cyclosporine A during long time frame experiments: relationship between pore opening and the activity of mitochondrial phospholipases. Biochemistry 34, 16440–16449.
Castilho, R.F., Kowaltowski, A.J., Vercesi, A.E., 1996. The irreversibility of inner mitochondrial membrane permeabilization by Ca^{2+} plus prooxidants is determined by

the extent of membrane protein thiol cross-linking. J. Bioenerg. Biomembr. 28, 523–539.
Chávez, E., Meléndez, E., Zazueta, C., Reyes-Vivas, H., Perales, S.G., 1997. Membrane permeability transition as induced by dysfunction of the electron transport chain. Biochem. Mol. Biol. Int. 41, 961–968.
Chinopoulos, C., Szabadkai, G., 2013. What makes you can also break you: mitochondrial permeability transition pore formation by the c subunit of the F_1F_0 ATP-synthase? Front. Oncol. 3, 25. http://dx.doi.org/10.3389/fonc.2013.00025.
Diwan, J.J., Lehrer, P.H., 1977. Inhibition of mitochondrial potassium ion flux by thallous ions. Biochem. Soc. Trans. 5, 203–205.
Elrod, J.W., Molkentin, J.D., 2013. Physiologic functions of cyclophilin D and the mitochondrial permeability transition pore. Circ. J. 77, 1111–1122.
Elustondo, P.A., Negoda, A., Kane, C.L., Kane, D.A., Pavlov, E.V., 2015. Spermine selectively inhibits high-conductance, but not low-conductance calcium-induced permeability transition pore. Biochim. Biophys. Acta 1847, 231–240.
Eskandari, M.R., Mashayekhi, V., Aslani, M., Hosseini, M.J., 2015. Toxicity of thallium on isolated rat liver mitochondria: the role of oxidative stress and MPT pore opening. Environ. Toxicol. 30, 232–241.
Foster, D.B., Ho, A.S., Rucker, J., Garlid, A.O., Chen, L., Sidor, A., Garlid, K.D., O'Rourke, B., 2012. Mitochondrial ROMK channel is a molecular component of mitoK_{ATP}. Circ. Res. 111, 446–454.
Galván-Arzate, S., Santamaría, A., 1998. Thallium toxicity. Toxicol. Lett. 99, 1–13.
Galván-Arzate, S., Pedraza-Chaverrí, J., Medina-Campos, O.N., Maldonado, P.D., Vázquez-Román, B., Ríos, C., Santamaría, A., 2005. Delayed effects of thallium in the rat brain: regional changes in lipid peroxidation and behavioral markers, but moderate alterations in antioxidants, after a single administration. Food Chem. Toxicol. 43, 1037–1045.
Gantner, N., Power, M., Babaluk, J.A., Reist, J.D., Köck, G., Lockhart, L.W., Solomon, K.R., Muir, D.C., 2009. Temporal trends of mercury, cesium, potassium, selenium, and thallium in Arctic char (*Salvelinus alpinus*) from Lake Hazen, Nunavut, Canada: effects of trophic position, size, and age. Environ. Toxicol. Chem. 28, 254–263.
García, N., Martínez-Abundis, E., Pavón, N., Chávez, E., 2007. On the opening of an insensitive cyclosporine A non-specific pore by phenylarsine plus mersalyl. Cell Biochem. Biophys. 49, 84–90.
Gehring, P.J., Hammond, P.B., 1967. The interrelationship between thallium and potassium in animals. J. Pharmacol. Exp. Ther. 155, 187–201.
Giorgio, V., Bisetto, E., Soriano, M.E., Dabbeni-Sala, F., Basso, E., Petronilli, V., Forte, M.A., Bernardi, P., Lippe, G., 2009. Cyclophilin D modulates mitochondrial F_0F_1-ATP synthase by interacting with the lateral stalk of the complex. J. Biol. Chem. 284, 33982–33988.
Giorgio, V., von Stockum, S., Antoniel, M., Fabbro, A., Fogolari, F., Forte, M., Glick, G.D., Petronilli, V., Zoratti, M., Szabó, I., Lippe, G., Bernardi, P., 2013. Dimers of mitochondrial ATP synthase form the permeability transition pore. Proc. Natl. Acad. Sci. U. S. A. 110, 5887–5892.
Gutiérrez-Aguilar, M., Baines, C.P., 2015. Structural mechanisms of cyclophilin D-dependent control of the mitochondrial permeability transition pore. Biochim. Biophys. Acta 1850, 2041–2047.
Halestrap, A.P., 2010. A pore way to die: the role of mitochondria in reperfusion injury and cardioprotection. Biochem. Soc. Trans. 38, 841–860.
Halestrap, A.P., Brenner, C., 2003. The adenine nucleotide translocase: a central component of the mitochondrial permeability transition pore and key player in cell death. Curr. Med. Chem. 10, 1507–1525.
Halestrap, A.P., Woodfield, K.Y., Connern, C.P., 1997. Oxidative stress, thiol reagents, and membrane potential modulate the mitochondrial permeability transition by affecting nucleotide binding to the adenine nucleotide translocase. J. Biol. Chem. 272, 3346–3354.
Hanzel, C.E., Verstraeten, S.V., 2006. Thallium induces hydrogen peroxide generation by impairing mitochondrial function. Toxicol. Appl. Pharmacol. 216, 485–492.
Hanzel, C.E., Verstraeten, S.V., 2009. Tl(I) and Tl(III) activate both mitochondrial and extrinsic pathways of apoptosis in rat pheochromocytoma (PC12) cells. Toxicol. Appl. Pharmacol. 236, 59–70.
Hashimoto, M., Majima, E., Goto, S., Shinohara, Y., Terada, H., 1999. Fluctuation of the first loop facing the matrix of the mitochondrial ADP/ATP carrier deduced from intermolecular cross-linking of Cys_{56} residues by bifunctional dimaleimides. Biochemistry 38, 1050–1056.
Herman, M.M., Bensch, K.G., 1967. Light and electron microscopic studies of acute and chronic thallium intoxication in rats. Toxicol. Appl. Pharmacol. 10, 199–222.
Hsieh, P.J., Su, H.Y., Lo, H.S., Chen, M.L., 2012. Dipyridamole ^{201}Tl myocardial SPECT in the assessment of a patient with myocardial bridging and concomitant atherosclerotic coronary artery disease. Clin. Nucl. Med. 37, e257–e262.
Kiliç, G.A., Kutlu, M., 2010. Effects of exogenous metallothionein against thallium-induced oxidative stress in rat liver. Food Chem. Toxicol. 48, 980–987.
Klingenberg, M., 2008. The ADP and ATP transport in mitochondria and its carrier. Biochim. Biophys. Acta 1778, 1978–2021.
Korotkov, S.M., 2009. Effects of Tl^+ on ion permeability, membrane potential and respiration of isolated rat liver mitochondria. J. Bioenerg. Biomembr. 41, 277–287.
Korotkov, S.M., 2016. Data Supporting the Involvement of the Adenine Nucleotide Translocase Conformation in Opening the Tl^+-Induced Permeability Transition Pore in Ca^{2+}-Loaded Rat Liver Mitochondria (Submitted in Data in Brief).
Korotkov, S.M., Saris, N.E., 2011. Influence of Tl^+ on mitochondrial permeability transition pore in Ca^{2+}-loaded rat liver mitochondria. J. Bioenerg. Biomembr. 43, 149–162.
Korotkov, S.M., Skulskii, I.A., Glazunov, V.V., 1998. Cd^{2+} effects on respiration and swelling of rat liver mitochondria were modified by monovalent cations. J. Inorg. Biochem. 70, 17–23.
Korotkov, S.M., Glazunov, V.V., Yagodina, O.V., 2007. Increase in the toxic effects of Tl^+ on isolated rat liver mitochondria in the presence of nonactin. J. Biochem. Mol. Toxicol. 21, 81–91.
Korotkov, S.M., Emel'yanova, L.V., Yagodina, O.V., 2008. Inorganic phosphate stimulates the toxic effects of Tl^+ in rat liver mitochondria. J. Biochem. Mol. Toxicol. 22, 148–157.
Korotkov, S.M., Nesterov, V.P., Brailovskaya, I.V., Furaev, V.V., Novozhilov, A.V., 2013. Tl^+ induces both cationic and transition pore permeability in the inner membrane of rat heart mitochondria. J. Bioenerg. Biomembr. 45, 531–539.
Korotkov, S.M., Brailovskaya, I.V., Kormilitsyn, B.N., Furaev, V.V., 2014a. Tl^+ showed negligible interaction with inner membrane sulfhydryl groups of rat liver mitochondria, but formed complexes with matrix proteins. J. Biochem. Mol. Toxicol. 28, 149–156.
Korotkov, S., Konovalova, S., Emelyanova, L., Brailovskaya, I., 2014b. Y^{3+}, La^{3+}, and some bivalent metals inhibited the opening of the Tl^+-induced permeability transition pore in Ca^{2+}-loaded rat liver mitochondria. J. Inorg. Biochem. 141, 1–9.
Korotkov, S.M., Brailovskaya, I.V., Shumakov, A.R., Emelyanova, L.V., 2015a. Closure of mitochondrial potassium channels favors opening of the Tl^+-induced permeability transition pore in Ca^{2+}-loaded rat liver mitochondria. J. Bioenerg. Biomembr. 47, 243–254.
Korotkov, S.M., Emelyanova, L.V., Konovalova, S.A., Brailovskaya, I.V., 2015b. Tl^+ induces the permeability transition pore in Ca^{2+}-loaded rat liver mitochondria energized by glutamate and malate. Toxicol. in Vitro 29, 1034–1041.
Korotkov, S.M., Konovalova, S.A., Brailovskaya, I.V., 2015c. Diamide accelerates opening of the Tl^+-induced permeability transition pore in Ca^{2+}-loaded rat liver mitochondria. Biochem. Biophys. Res. Commun. 468, 360–364.
Kowaltowski, A.J., Castilho, R.F., 1997. Ca^{2+} acting at the external side of the inner mitochondrial membrane can stimulate mitochondrial permeability transition induced by phenylarsine oxide. Biochim. Biophys. Acta 1322, 221–229.
Kowaltowski, A.J., Vercesi, A.E., Castilho, R.F., 1997. Mitochondrial membrane protein thiol reactivity with N-ethylmaleimide or mersalyl is modified by Ca^{2+}: correlation with mitochondrial permeability transition. Biochim. Biophys. Acta 1318, 395–402.
Lapidus, R.G., Sokolove, P.M., 1994. The mitochondrial permeability transition. interactions of spermine, ADP, and inorganic phosphate. J. Biol. Chem. 269, 18931–18936.
Leung, K.M., Ooi, V.E., 2000. Studies on thallium toxicity, its tissue distribution and histopathological effects in rats. Chemosphere 41, 155–159.
Li, Y., Johnson, N., Capano, M., Edwards, M., Crompton, M., 2004. Cyclophilin-D promotes the mitochondrial permeability transition but has opposite effects on apoptosis and necrosis. Biochem. J. 383, 101–109.
Li, S., Huang, W., Duan, Y., Xing, J., Zhou, Y., 2015. Human fatality due to thallium poisoning: autopsy, microscopy, and mass spectrometry assays. J. Forensic Sci. 60, 247–251.
Lopatin, A.N., Makhina, E.N., Nichols, C.G., 1998. A novel crystallization method for visualizing the membrane localization of potassium channels. Biophys. J. 74, 2159–2170.
Lu, T., Wu, L., Xiao, J., Yang, J., 2001. Permeant ion-dependent changes in gating of Kir2.1 inward rectifier potassium channels. J. Gen. Physiol. 118, 509–521.
Majima, E., Koike, H., Hong, Y.M., Shinohara, Y., Terada, H., 1993. Characterization of cysteine residues of mitochondrial ADP/ATP carrier with the SH-reagents eosin 5-maleimide and N-ethylmaleimide. J. Biol. Chem. 268, 22181–22187.
Mauerer, U.R., Boulpaep, E.L., Segal, A.S., 1998. Properties of an inwardly rectifying ATP-sensitive K^+ channel in the basolateral membrane of renal proximal tubule. J. Gen. Physiol. 111, 139–160.
McStay, G.P., Clarke, S.J., Halestrap, A.P., 2002. Role of critical thiol groups on the matrix surface of the adenine nucleotide translocase in the mechanism of the mitochondrial permeability transition pore. Biochem. J. 367, 541–548.
Melnick, R.L., Monti, L.G., Motzkin, S.M., 1976. Uncoupling of mitochondrial oxidative phosphorylation by thallium. Biochem. Biophys. Res. Commun. 69, 68–73.
Mitchell, P., Moyle, J., 1969. Translocation of some anions cations and acids in rat liver mitochondria. Eur. J. Biochem. 9, 149–155.
Mulkey, J.P., Oehme, F.W., 1993. A review of thallium toxicity. Vet. Hum. Toxicol. 35, 445–453.
Nantes, I.L., Rodrigues, T., Caires, A.C., Cunha, R.L., Pessoto, F.S., Yokomizo, C.H., Araujo-Chaves, J.C., Faria, P.A., Santana, D.P., dos Santos, C.G., 2011. Specific effects of reactive thiol drugs on mitochondrial bioenergetics. J. Bioenerg. Biomembr. 43, 11–18.
Ogata, M., Mori, T., Izushi, F., Etoh, K., Sakai, R., Meguro, T., Inoue, B., 1983. Classification of potentially toxic chemicals based on their effects on mitochondrial respiration. Physiol. Chem. Phys. Med. NMR 15, 229–232.
Perrin, D.D., 1979. Stability Constants of Metal-Ion Complexes. Part B. Organic Ligands. Pergamon, Oxford.
Peter, A.L., Viraraghavan, T., 2005. Thallium: a review of public health and environmental concerns. Environ. Int. 31, 493–501.
Petronilli, V., Costantini, P., Scorrano, L., Colonna, R., Passamonti, S., Bernardi, P., 1994. The voltage sensor of the mitochondrial permeability transition pore is tuned by the oxidation–reduction state of vicinal thiols. Increase of the gating potential by oxidants and its reversal by reducing agents. J. Biol. Chem. 269, 16638–16642.
Petronilli, V., Sileikyte, J., Zulian, A., Dabbeni-Sala, F., Jori, G., Gobbo, S., Tognon, G., Nikolov, P., Bernardi, P., Ricchelli, F., 2009. Switch from inhibition to activation of the mitochondrial permeability transition during hematoporphyrin-mediated photooxidative stress. Unmasking pore-regulating external thiols. Biochim. Biophys. Acta 1787, 897–904.
Pourahmad, J., Eskandari, M.R., Daraei, B., 2010. A comparison of hepatocyte cytotoxic mechanisms for thallium (I) and thallium (III). Environ. Toxicol. 25, 456–467.
Ramsden, D.B., 2007. Thallium. In: Waring, R.H., Steventon, G.B., Mitchell, S.C. (Eds.), Molecules of Death (2nd). Imperial College Press, London, UK, pp. 415–422.
Ricchelli, F., Sileikytė, J., Bernardi, P., 2011. Shedding light on the mitochondrial permeability transition. Biochim. Biophys. Acta 1807, 482–490.
Rigobello, M.P., Turcato, F., Bindoli, A., 1995. Inhibition of rat liver mitochondrial permeability transition by respiratory substrates. Arch. Biochem. Biophys. 319, 225–230.
Riley, M.V., Lehninger, A.L., 1964. Changes in sulfhydryl groups of rat liver mitochondria during swelling and contraction. J. Biol. Chem. 239, 2083–2089.

Riley Jr., W.W., Pfeiffer, D.R., 1985. Relationships between Ca^{2+} release, Ca^{2+} cycling, and Ca^{2+}-mediated permeability changes in mitochondria. J. Biol. Chem. 260, 12416–12425.

Rodríguez-Mercado, J.J., Altamirano-Lozano, M.A., 2013. Genetic toxicology of thallium: a review. Drug Chem. Toxicol. 36, 369–383.

Salvi, M., Battaglia, V., Brunati, A.M., La Rocca, N., Tibaldi, E., Pietrangeli, P., Marcocci, L., Mondovì, B., Rossi, C.A., Toninello, A., 2007. Catalase takes part in rat liver mitochondria oxidative stress defense. J. Biol. Chem. 282, 24407–24415.

Saris, N.E., Skulskii, I.A., Savina, M.V., Glasunov, V.V., 1981. Mechanism of mitochondrial transport of thallous ions. J. Bioenerg. Biomembr. 13, 51–59.

Schoer, J., 1984. Thallium. In: Hutzinger, O. (Ed.), Handbook of Environmental Chemistry. Anthropogenic Compounds. Springer, New York, pp. 143–214.

Singh, B.K., Tripathi, M., Pandey, P.K., Kakkar, P., 2011. Alteration in mitochondrial thiol enhances calcium ion dependent membrane permeability transition and dysfunction in vitro: a cross-talk between mtThiol, Ca^{2+}, and ROS. Mol. Cell. Biochem. 357, 373–385.

Villaverde, M.S., Hanzel, C.E., Verstraeten, S.V., 2004. In vitro interactions of thallium with components of the glutathione-dependent antioxidant defence system. Free Radic. Res. 38, 977–984.

Waldmeier, P.C., Feldtrauer, J.J., Qian, T., Lemasters, J., 2002. Inhibition of the mitochondrial permeability transition by the nonimmunosuppressive cyclosporine derivative NIM811. Mol. Pharmacol. 62, 22–29.

Wojtovich, A.P., Williams, D.M., Karcz, M.K., Lopes, C.M., Gray, D.A., Nehrke, K.W., Brookes, P.S., 2010. A novel mitochondrial K_{ATP} channel assay. Circ. Res. 106, 1190–1196.

Woods, J.S., Fowler, B.A., 1986. Alteration of hepatocellular structure and function by thallium chloride: ultrastructural, morphometric, and biochemical studies. Toxicol. Appl. Pharmacol. 83, 218–229.

Zazueta, C., Sánchez, C., García, N., Correa, F., 2000. Possible involvement of the adenine nucleotide translocase in the activation of the permeability transition pore induced by cadmium. Int. J. Biochem. Cell Biol. 32, 1093–1101.

Zierold, K., 2000. Heavy metal cytotoxicity studied by electron probe X-ray microanalysis of cultured rat hepatocytes. Toxicol. in Vitro 14, 557–563.

Zoccarato, F., Rugolo, M., Siliprandi, D., Siliprandi, N., 1981. Correlated effluxes of adenine nucleotides, Mg^{2+} and Ca^{2+} induced in rat-liver mitochondria by external Ca^{2+} and phosphate. Eur. J. Biochem. 114, 195–199.